AD-A093 045 UNITED TECHNOLOGIES RESEARCH CENTER EAST HARTFORD CONN F/G 20/5
PULSED SUBMILLIMETER LASER PROGRAM.(U)
MAY 79 L M LAUGHMAN, L A NEWMAN, R J WAYNE DAAB07-77-C-2177
UNCLASSIFIED UTRC/R79-922991-17 NL

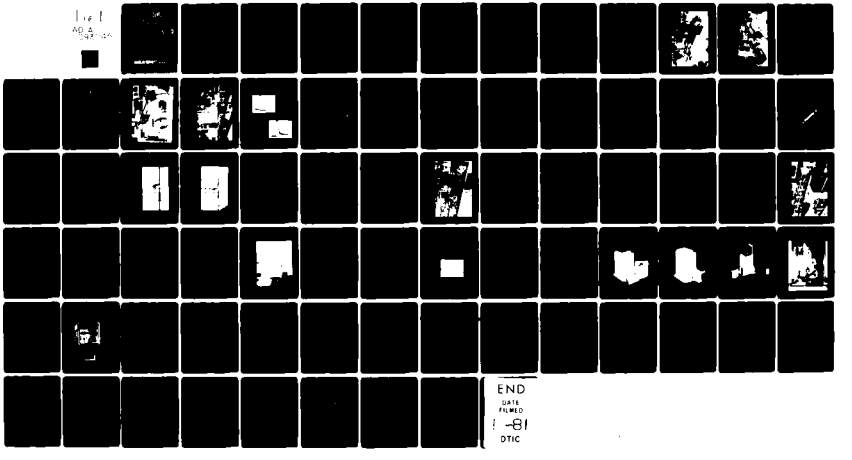

END
DATE FILMED
1-81
DTIC

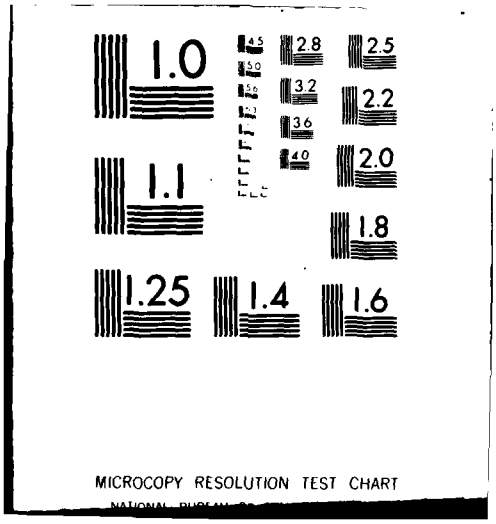
1.0
1.1
1.25
1.4
1.6
1.8
2.0
2.2
2.5
2.8
3.2
3.6
4.0
4.5
5.0
5.6
MICROCOPY RESOLUTION TEST CHART

R922991-17

LEVEL II

Pulsed Submillimeter Laser Program.

UTRC/R79-922991-17

by:

L.M. Laughman
L.A. Newman
R.J. Wayne

Contract DAAB07-77-C-2177

30 August 1977 through 15 May 1979

12 75

FINAL TECHNICAL REPORT.
30 Aug 77 - 15 May 79,

UNITED TECHNOLOGIES
RESEARCH CENTER
EAST HARTFORD, CONNECTICUT 06108

R79-922991-17

Pulsed Submillimeter Laser Program

TABLE OF CONTENTS

LIST OF FIGURES

LIST OF FIGURES (Cont'd)

LIST OF FIGURES (Cont'd)

R79-922991-17

Pulsed Submillimeter Laser Program

1.0 INTRODUCTION

This report describes the results of an exploratory development program to investigate various system and component aspects of a pulsed FIR heterodyning laser radar. This work was conducted by United Technologies Research Center (UTRC) during the period 30 August 1977 and 31 May 1979.

During the course of this developmental program a number of interrelated subsystems required for a heterodyning FIR radar were investigated. The work focused on optically pumped FIR lasers which utilize a CO_2 laser pump source. Pulsed FIR and CO_2 pump lasers are required for the primary radar transmitter, and CW FIR and CO_2 lasers are needed for the laser radar local oscillator. The transversely excited (TE) CO_2 laser which serves as the pulsed FIR laser pump is itself a central component of the radar system and the performance characteristics of a recirculating, high pulse repetition frequency (PRF) TE CO_2 as a FIR pump were experimentally examined. A number of different pulsed FIR laser resonators were investigated with the objective of minimizing system size. The requirement for a stable FIR local oscillator imposes certain constraints on the CW CO_2 pump source and a stable single mode CO_2 pump source has been designed and characterized. A sealed-off CW FIR laser with an Invar stabilized cavity was constructed for use as a local oscillator source. A number of detectors for use at submillimeter wavelength were examined and pulsed and CW detection with two micron Schottky diodes were performed.

Because of the extreme sensitivity of the CW FIR laser and pump source to temperature fluctuation a technique for stabilizing the CO_2 utilizing the photoacoustic effect in the FIR medium was examined and found to be very promising.

2.0 SYSTEM OVERVIEW

A heterodyning submillimeter wave radar transceiver necessarily includes the following components: (1) pulsed FIR laser; (2) pulsed CO_2 laser pump; (3) CW FIR laser; (4) CW CO_2 laser pump; (5) FIR mixer-detector; (6) transmitter and local oscillator frequency stabilization control loops. A schematic layout of the lasers and detector is shown in Fig. 1. Each of the components listed above is in itself a subsystem of considerable complexity. As the current program evolved it became clear that any serious effort to construct an FIR radar must be preceded by a phase in which the various subsystems are developed and parameterized. The direction of the program accordingly moved toward addressing the development of the laser and detector subsystems and identifying those areas in need of additional research.

Summarized below are the areas in which the Pulsed Submillimeter Laser Program efforts were concentrated, and why these particular topics required a focused R&D effort.

The pulsed discharge TE CO_2 laser serves as the optical pumping source for the pulsed submillimeter transmitter. With typical 10μm to FIR conversion efficiencies of less than 1 percent, the TE CO_2 must have a pulse energy 100 mJ or greater. Maximum PRF's of up to 1 KHz are of interest for radar applications and thus the TE pump becomes a device of up to several hundred watts average power with peak pulse powers in the megawatt range. UTRC has for some years conducted a program of research and development in the area of high PRF TE CO_2 lasers and one such device (Ref. 1) was utilized as the pulsed FIR pump source in this program. In addition to using the existing laser as an FIR pump, a number of questions concerning TE CO_2 laser development as it relates to FIR laser pumping were addressed within the scope of the current program. These areas include: frequency stability; transverse mode purity; discharge circuit design; high PRF beam quality; gas chemistry changes at high PRF.

Because there are no pulsed discharge considerations the pulsed FIR laser is a relatively simple device compared to the TE CO_2 laser. The principal issues involve resonator design, frequency stability and laser linewidth, and vacuum structure design. Both 496 μm and 944 μm pulsed laser outputs were obtained and observed with high-speed detectors, and several resonator configurations were tested. The energy per pulse of the CH_3F laser at 496 μm was also examined at PRF's to 350 Hz.

The CW local oscillator FIR laser and the associated CW CO_2 pump form a subsystem analogous to the pulsed-laser pair. The development of the CW laser emphasized frequency stability and mode purity for three reasons: first, a

FIG. 1

FIR EXPERIMENTAL LAYOUT

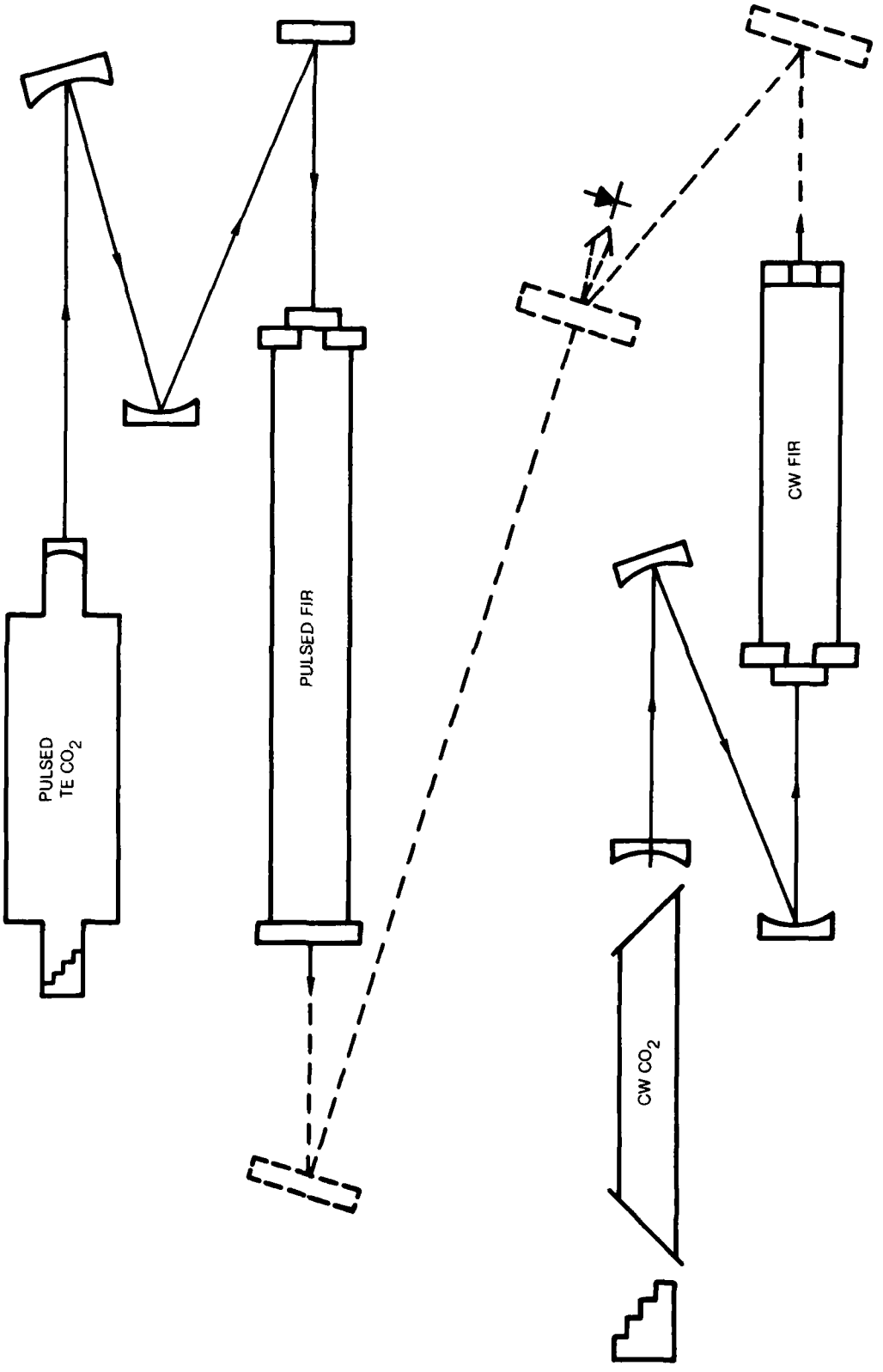

79–10–130–10

frequency stable local oscillator is a fundamental prerequisite for a heterodyning radar which can exploit the signal-to-noise ratio enhancement which is made possible by a narrow receiver bandwidth; second, the CW laser serves as a somewhat simpler testbed which can be used to develop techniques applicable to the pulsed laser system; third, the availability of a stable CW FIR laser permits a more detailed characterization of FIR detectors. Issues addressed in the course of the program include the following: (1) CW FIR resonator design; (2) sealed-off FIR laser structure design; (3) CW CO_2 laser design; (4) CO_2 laser frequency stabilization by optoacoustic absorption technique.

Several different devices were initially considered as candidate submillimeter wave detectors. The fast response and high sensitivity of Schottky diodes indicated fairly early in the program that this would be the detector of choice provided devices with response to 600 GHz could be obtained. A number of detectors were obtained and tested with pulsed and CW FIR outputs at 496 m and 944 m. The sensitivity of the small area diodes to RFI induced currents was identified as an issue as a result of the proximity of the pulsed CO_2 TE laser and an RFI shielded detector module was developed.

Figures 2 and 3 show the laboratory setup for both pulsed and CW FIR lasers and their respective pump sources. The individual elements of the system will be discussed in detail in the following section.

FIG. 2

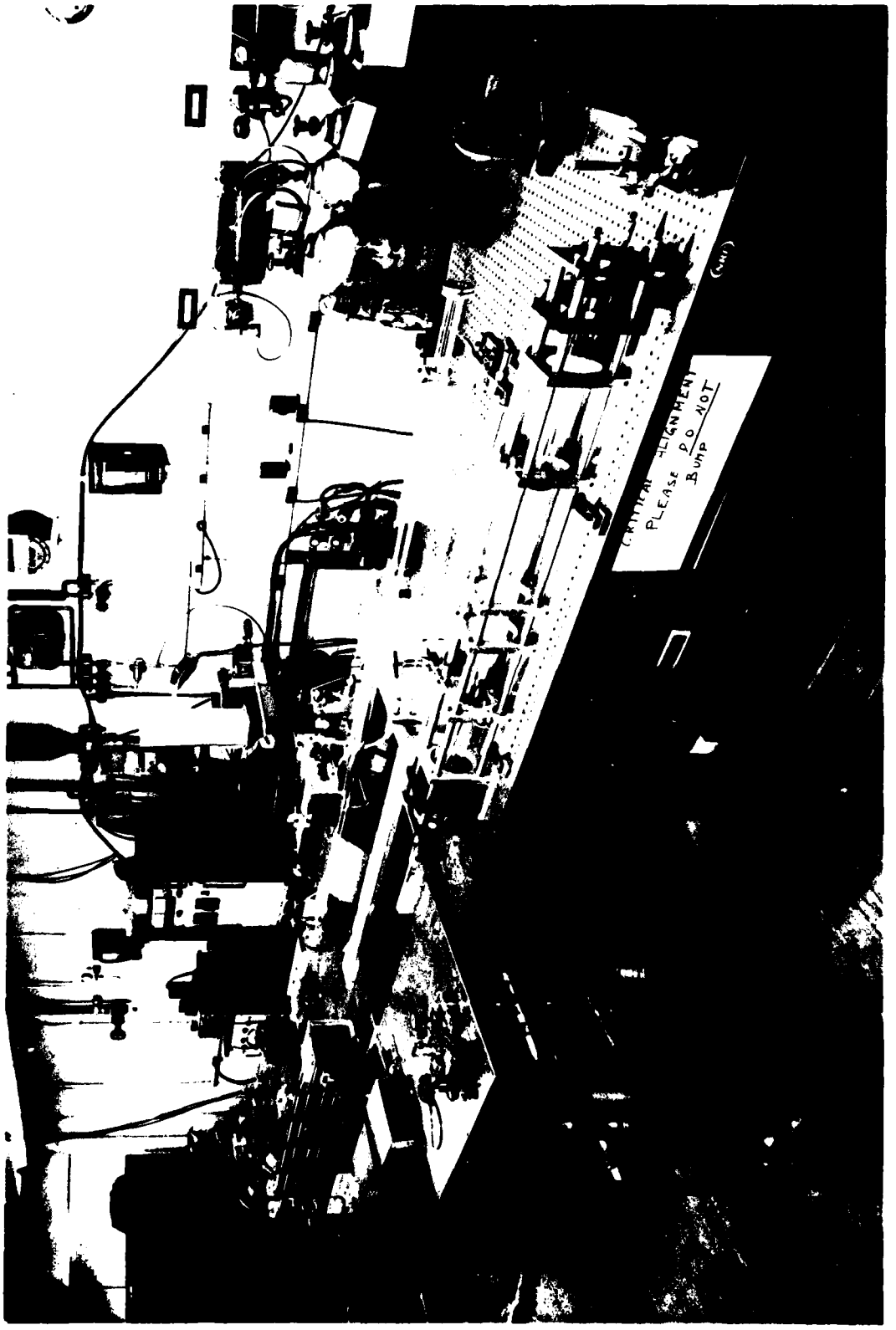

FIR EXPERIMENTAL LAYOUT

79 10 130 26

FIG. 3

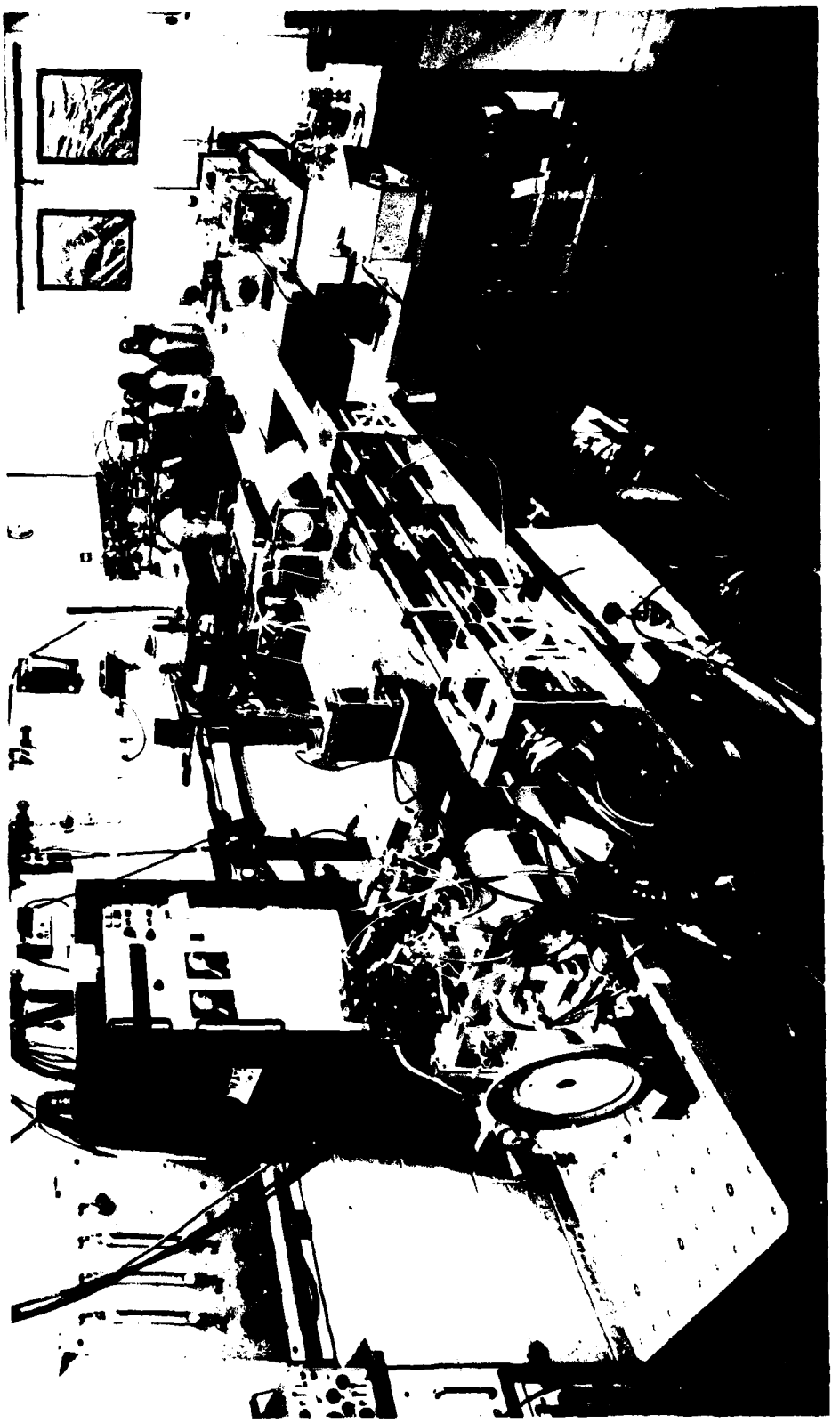

FIR EXPERIMENTAL LAYOUT

79-10-130-24

3.0 LASER AND RECEIVER SUBSYSTEM

In this section each of the subsystems which were the subjects of this investigation are discussed. Design features as well as experimental methods and results for pulsed and CW lasers, and the FIR receiver are presented.

3.1 Pulsed CO_2 TE Pump Laser

The design of a high PRF, high output energy laser oscillator requires the integration of a suitable pulsed discharge geometry, a high volume recirculating blower, heat exchanger, and appropriate gas ducting. Reference 1 describes work performed at UTRC which culminated in the demonstration of TE CO_2 laser operation at 1 KHz PRF with an average power of 860 W. This basic laser was utilized on the pulsed FIR laser pump, but certain refinements of a basic multimode laser are necessary to optimize it as an FIR pump source. Figure 4 summarizes the characteristics of the TE CO_2 laser as it existed at the beginning of the program and modifications needed for FIR pump applications. The significance of these modifications is that they invariably tend to reduce laser power and increase laser size and weight, both of which have obvious implications for realistic estimates of FIR radar system dimensions. The TE CO_2 laser is based on the gas circulator and discharge head shown in Fig. 5. When configured as a multimode, high power laser the total laser structure as shown in Fig. 6 is not substantially larger than the recirculator assembly. However, in this configuration the vibrational inputs of the blower to the optical elements introduce a source of great frequency instability and the result on the pulsed FIR output is amplitude fluctuations. In order to isolate the optical elements from vibrational inputs the gas circulator is isolated from the optical mounting surfaces by flexible, vacuum tight diaphragms. This arrangement is shown in Fig. 7. The optical mounts are referenced to optical tables which are coupled to the gas circulator only through their common use of the laboratory floor. Intravacuum optics were used for the TE laser in order to avoid the optical damage problems and transverse mode degradation which often accompany the use of Brewster windows.

The PRF and pulse energy of the TE CO_2 laser were originally maximized at a pressure of 250 torr. At this pressure the optical pulse has a relatively long "tail" lasting in excess of 20 μs and containing most of the pulse energy. A typical pulse shape is shown in Fig. 8. This pulse is not efficient for pumping a FIR inversion because of the very short upper level lifetime in the FIR gain medium which generally has maximum gain with a medium pressure on the order of one torr. Even for high energy pump pulses of this shape, the pulse tail is too weak to raise the FIR laser above threshold. The pulse can be shortened to a certain extent by operating at a higher TE laser pressure. Figure 9 illustrates the effect on optical shape of raising laser pressure. It can be seen that considerable pulse shortening occurs as the pressure is raised from

TE CO_2 PUMP SOURCE

- INITIAL CHARACTERISTICS
  - 1 JOULE, MULTIMODE: 1KHz PRF
  - 250 TORR
  - LOW GAIN, 5% OUTPUT COUPLING, NO GRATING
  - RESONATOR ELEMENTS NOT VIBRATIONALLY ISOLATED FROM GAS RECIRCULATOR
  - 150 J/LITER ATM SPECIFIC INPUT

- REQUIRED PERFORMANCE
  - SHORTER PULSE, HIGHER PRESSURE AND/OR REDUCED N_2
    - * RETUNING L-R-C DISCHARGE ELEMENTS
    - * GAS CHEMISTRY CHANGES LIMIT SPECIFIC INPUT AT HIGHER PRESSURE AND HIGHER PRF
    - * REDUCE ELECTRODE WIDTH TO MATCH TEM_{00} MODE AND MAXIMIZE USEFUL ENERGY INPUT
  - * DECOUPLE OPTICS FROM RECIRCULATOR VIBRATION
    SINGLE MODE OUTPUT
    GRATING CONTROL — INTRAVACUUM OPTICS*
    1 KHz BEAM QUALITY

* ITEMS SIGNIFICANTLY AFFECTED BY $\gtrsim$100 Hz OPERATION

FIG. 5

PULSED LASER TRANSMITTER DIMENSIONAL DATA

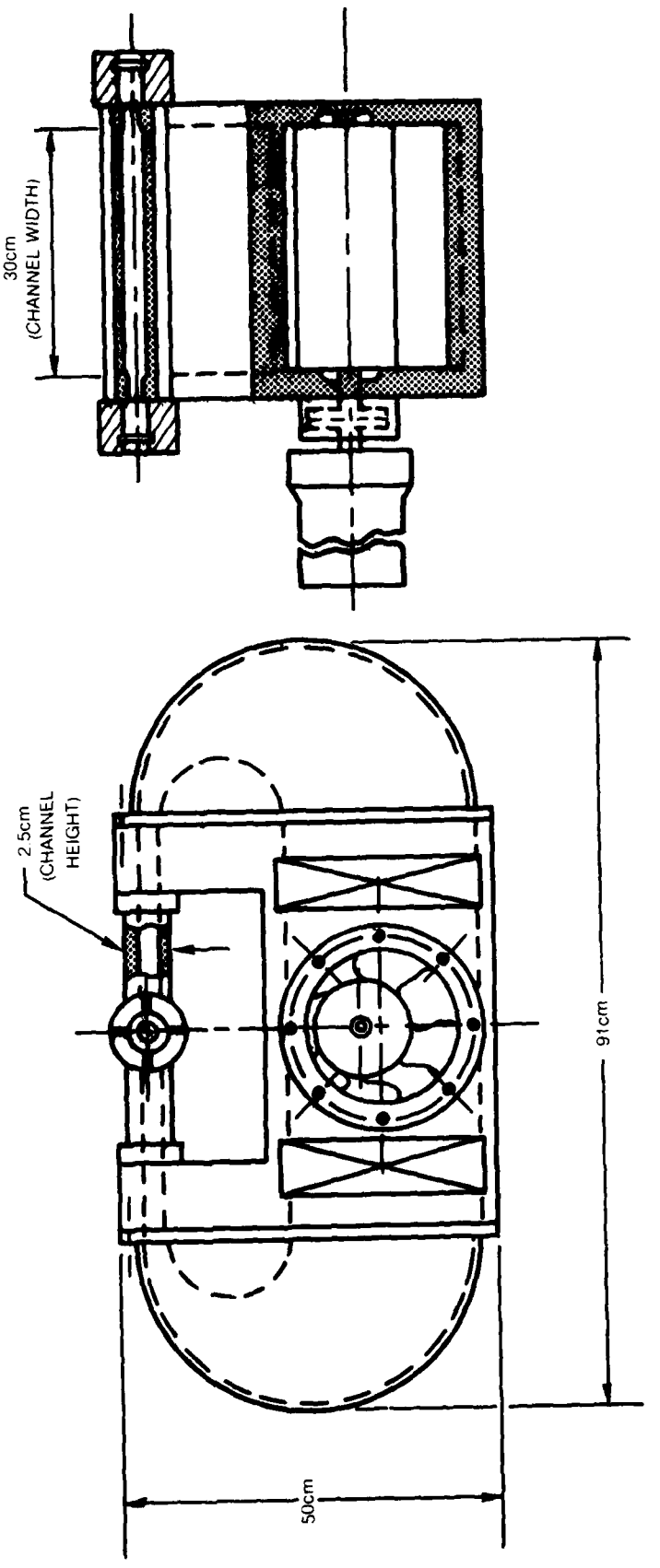

79-10-130-9

FIG. 6

PULSED LASER TRANSMITTER

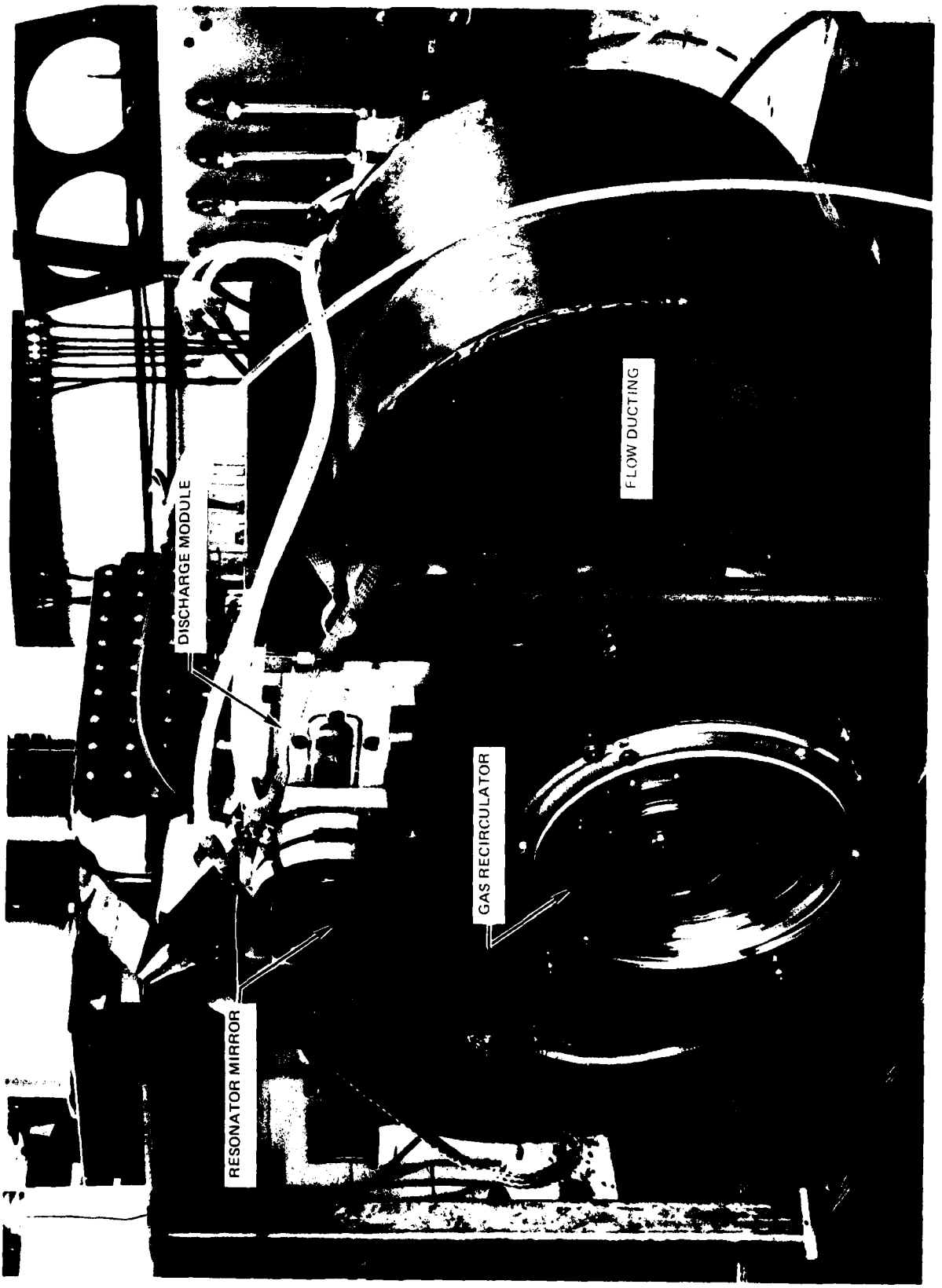

77-08-216-1

FIG. 7

TE CO_2 LASER WITH VIBRATIONALLY DECOUPLED RESONATOR

OPTICAL PULSE FOR 5% OUTPUT COUPLING AND CO_2 :N_2 :He = 1 :0.46 :4.1

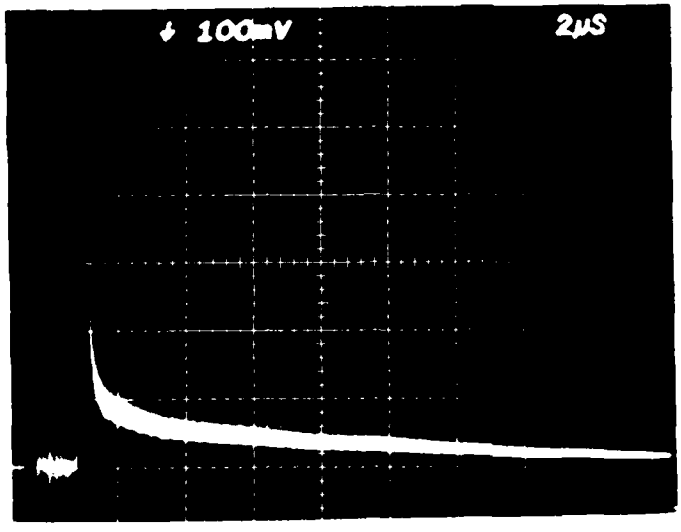

a.
GAIN–SWITCHED SPIKE
PLUS RELAXED PULSE

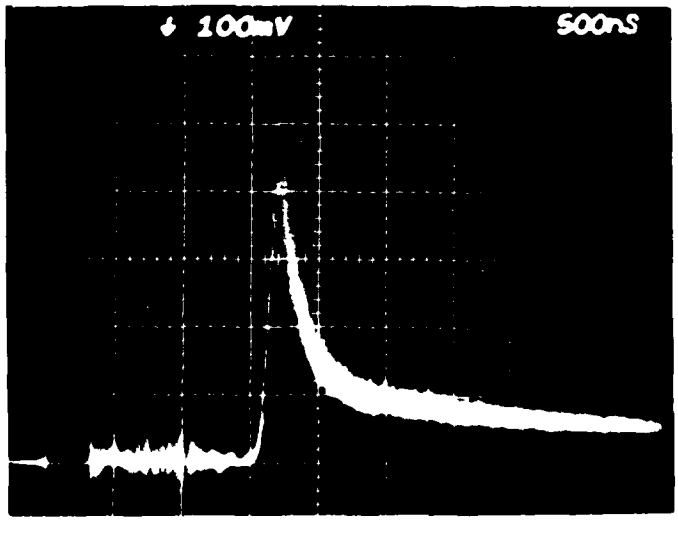

b.
DETAIL OF GAIN–SWITCHED
SPIKE

FIG. 9

PRESURE DEPENDENCE OF PULSE WIDTH

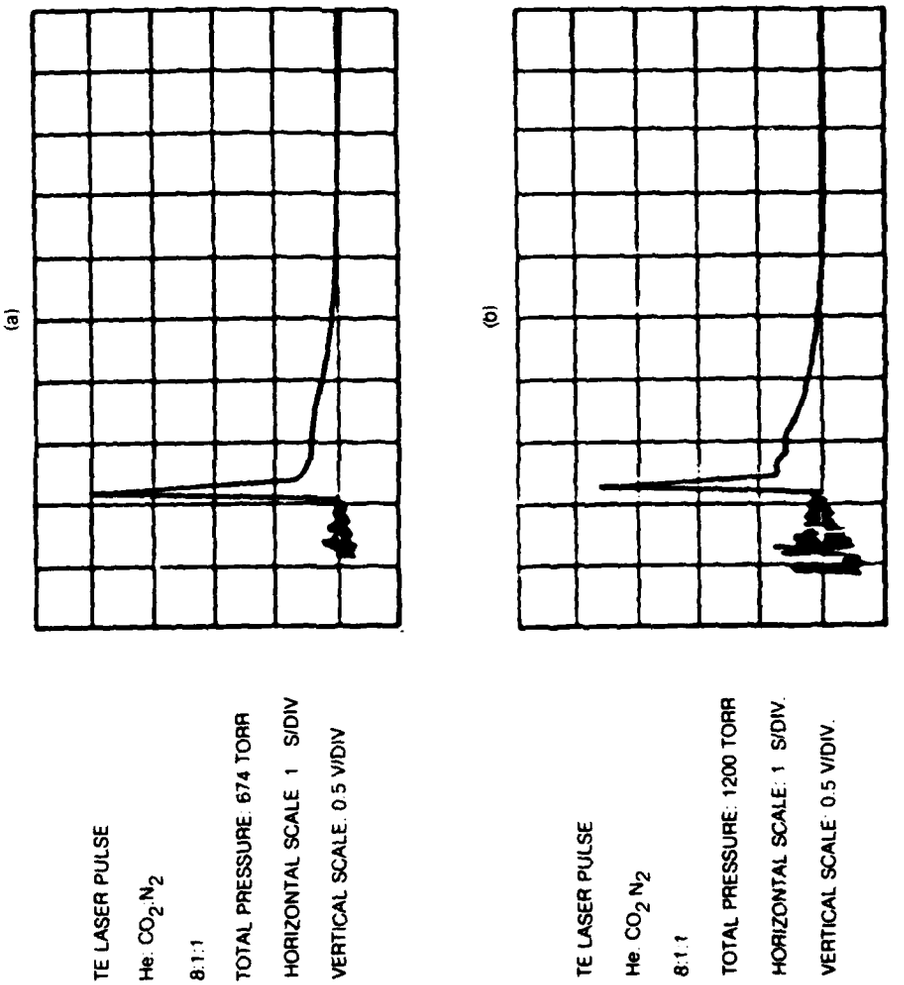

79-08-127-1

250 torr to 674 torr, but very little further improvement is obtained by going to 1200 torr. Nearly total elimination of the pulse tail is effected by using only He and CO_2 as shown in Fig. 10, but this has the substantial disadvantage of reducing the energy within the gain switched spike (within the first 500 ns) by nearby a factor of two from the spike energy obtained with nitrogen. Thus although only the energy in the gain switched spike is effective as pump energy it is worthwhile to use N_2 containing mixes. The pulse shortening due to pressure increase saturates at approximately 400 torr and further pulse shortening occurs very slowly with increasing pressure, thus a working pressure of 400-500 torr was determined as most suitable for the FIR pump. There is a distinct advantage in operating a recirculating TE CO_2 laser at less than atmospheric pressure as a result of the gas chemistry changes which occur in sealed-off or limited gas makeup conditions. The buildup of CO and O_2 in recirculating TE CO_2 lasers is well known and avoidance of the attendent discharge arcing has been discussed by several authors (Ref. 2). We have found that lower pressure operation substantially increases the maximum PRF which can be sustained without arcing. For example a gas makeup rate which can support atmospheric pressure operation at only 50 Hz can support a PRF of several hundred Hz at 250 torr. The optimum CO_2 pressure is therefore the lowest which yields the shorter optical pulse, i.e. 400-500 torr.

Efficient operation of the CO_2 TE laser dictates that the optical mode volume should match the TE laser gain volume. As originally configured for a 1 J pulse energy the TE gain volume was 2 cm x 4 cm x 20 cm long. The Fresnel number for this gain medium is approximately 300 and since there is not sufficient gain to support efficient unstable resonator operation the resonator must be apertured and/or lengthened to achieve an optical Fresnel number of five or less, a range in which single transverse mode operation of a TE CO_2 laser has been achieved. For the purposes of this program the optical cavity was lengthened to greater than one meter and the optical volume was defined by a 1 cm aperture. When a grating rotational line selector is used as one end mirror, the single transverse mode laser produced 100-150 mJ vs. the 1.1 J maximum multimode energy. The available single mode energy could be improved by perhaps a factor of two by using a multipass resonator to increase the effective mode volume, however this additional refinement was not deemed necessary for the purposes of the Pulsed Submillimeter Laser Program. This reduction in energy and increase in laser size appears to be typical of the penalty paid in going from a multimode laser to a single-mode laser and will accordingly have a significant impact on the design of any FIR radar which incorporates a pulsed TE CO_2 laser.

The beam quality of the TE CO_2 laser could possibly degrade at higher PRF's as a result of severe acoustic perturbations of the optical medium. Such effects have been observed in high average power CO_2 and chemical lasers, and in the TE CO_2 laser acoustic perturbations of the amplitude and frequency of the optical pulse can often be observed within a few microseconds of the discharge (Ref. 3). At high PRF's, i.e. greater than a few hundred hertz, the

FIG. 10

OPTICAL PULSE SHAPE FOR He: CO_2:N_2 = 8:1:0

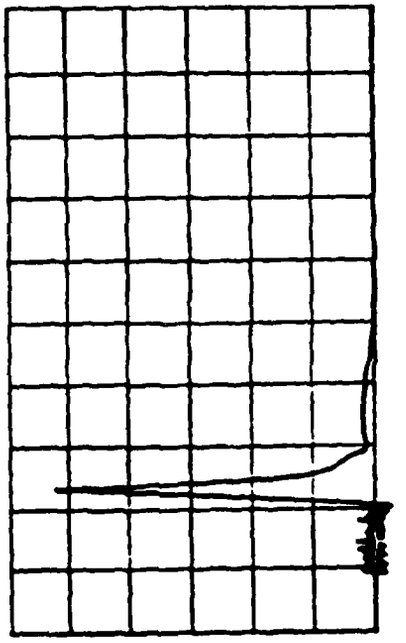

TE LASER PULSE: He:CO_2:N_2:8:1:0

TOTAL PRESSURE: 850 TORR

HORIZONTAL SCALE: 0.5 S/DIV.

VERTICAL SCALE: 0.5 V/DIV.

79-09-127-2

acoustic shock wave may persist through the interpulse period with enough strength to reduce the energy and/or transverse mode purity of subsequent pulses. In Ref. 1 the question of energy reduction due to high PRF acoustics was specifically examined and determined not to be a problem, but the more subtle effects on beam quality have not until now been investigated. Since the presence of such perturbations could have a significant impact on a submillimeter radar an experiment to determine beam quality in the 100 Hz-1 KHz range was undertaken.

The TE laser cavity was set up as a partially transmitting unstable resonator in order to achieve a high purity, single transverse mode at lower PRF's. The following measurements were also made using a stable resonator with no significant change in the outcome. Figure 11 shows the experimental arrangement for the high PRF beam quality test. The output of the laser resonator was focused through a calibrated aperture and the transmitted power was compared to the power expected for a single mode oscillator. Data were taken with a clearing ratio of 1 to 1.5, that is the gas in the discharge volume was change 1 to 1.5 times between pulses. This relatively low clearing ratio will emphasize the effects of acoustic disturbances whereas higher clearing ratios will reduce the interpulse acoustic effects. The low PRF (100 Hz) beam quality is shown in Fig. 12 where the solid curve is the Airy function expected from the idealized unstable resonator and the circles are the experimentally measured transmitted power. The match is obviously quite good and we may therefore presume that single mode, diffraction-limited performance is demonstrated at 100 Hz. Figure 13 presents the power through three different aperture sizes as a function of PRF from 100 Hz to 1000 Hz. There is no statistically significant variation in transmitted power over this range of PRF's and it may therefore be concluded that whatever acoustic disturbances persist through the interpulse period are insufficient to produce any significant degradation of the output beam quality. Operation of a high PRF submillimeter wave radar involves many fundamental technical issues, but it now appears that degradation of the TE CO_2 pump source at high PRF's will in no way limit the pulsed FIR output.

3.2 Pulsed Submillimeter Wave Laser

The pulsed FIR laser consists of a passive optically pumped gain medium and resonator elements with provision for coupling in the pump radiation and coupling out the FIR radiation with a minimum of interference between the two processes. Figure 14 illustrates the most commonly used input and output optical configurations used for pulsed FIR lasers, and the four resonator configurations implied by Fig. 14 have been tried in the present program.

Since compactness of the laser system is a continuing concern we initially investigated a 1 meter gain cell for the pulsed FIR laser. This device is shown in Fig. 15. Both collimated and focused input beams were tried and both

FIG. 11

BEAM QUALITY DIAGNOSIS EXPERIMENT

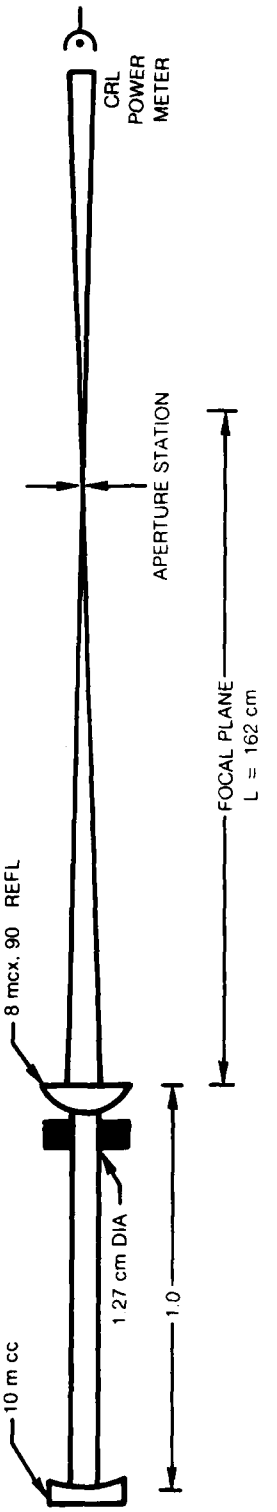

RESONATOR PARAMETERS

M = 1.25 POSITIVE BRANCH u/o
N_T = 5.9
N_{eq} = 0.48

MEDIUM PARAMETERS

GAS PRESSURE 500 TORR
ENERGY LOADING ≅ 100 J/L-A
PULSE WIDTH ≅ 1.5 μs
CLEARING RATIO ≅ 1

79-10-130-15

FIG. 12

PULSED RECIRCULATING TE LASER BEAM QUALITY WITH PARTIALLY TRANSMITTING UNSTABLE RESONATOR

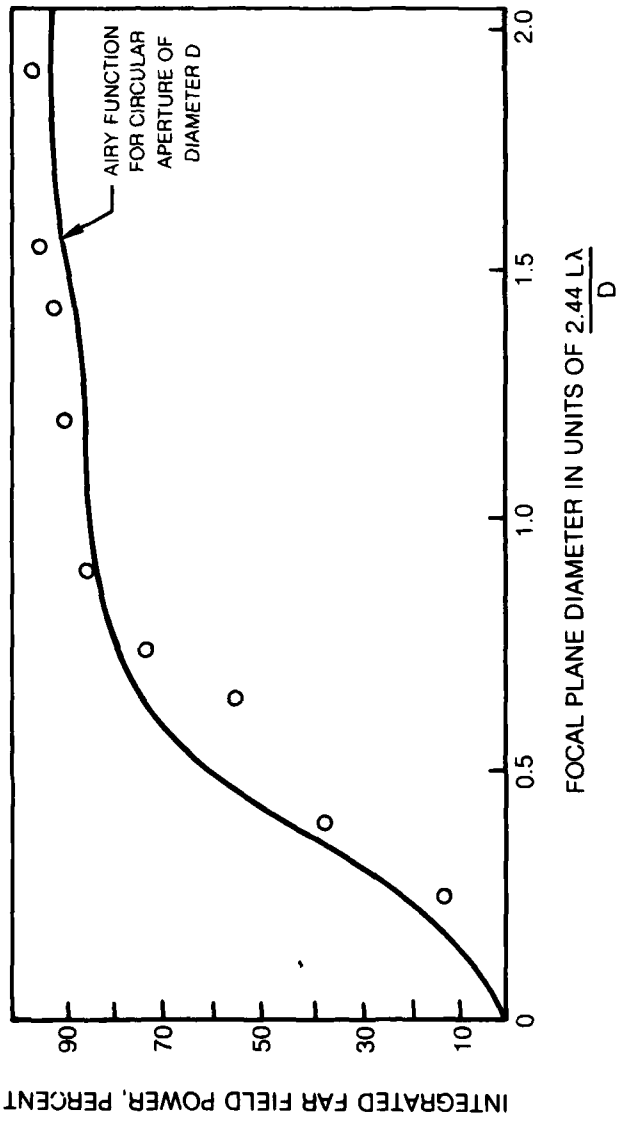

79-10-130-11

FIG. 13

PULSED RECIRCULATING TE LASER BEAM QUALITY WITH PARTIALLY TRANSMITTING UNSTABLE RESONATOR

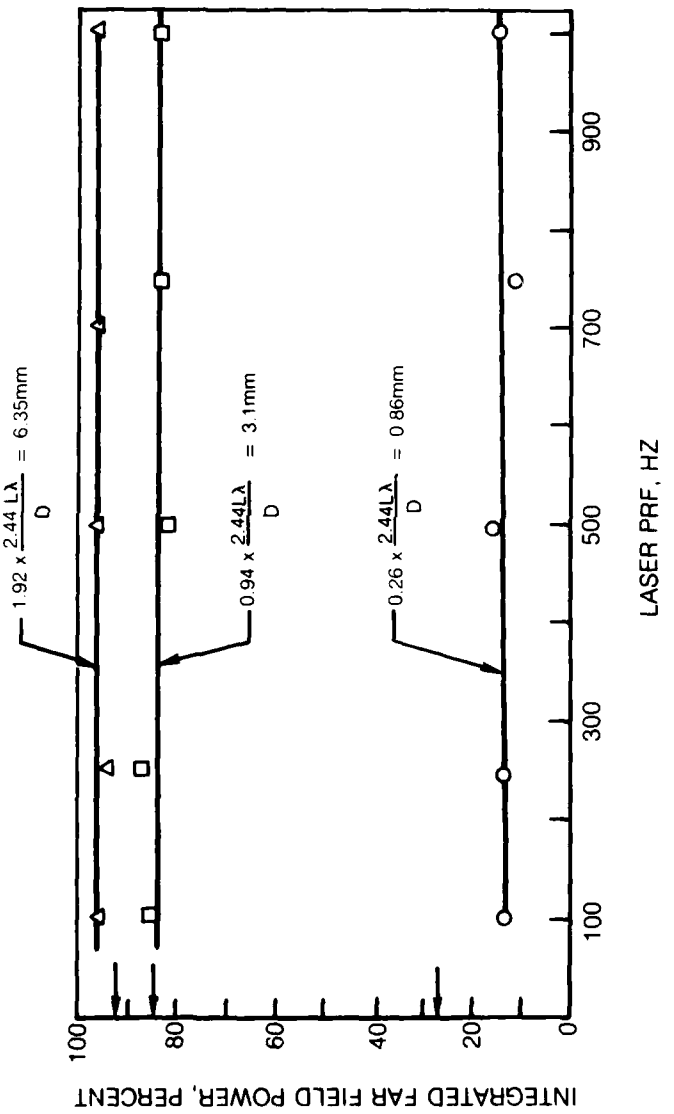

79-10-130-12

FIG. 14

PULSED FIR CAVITIES

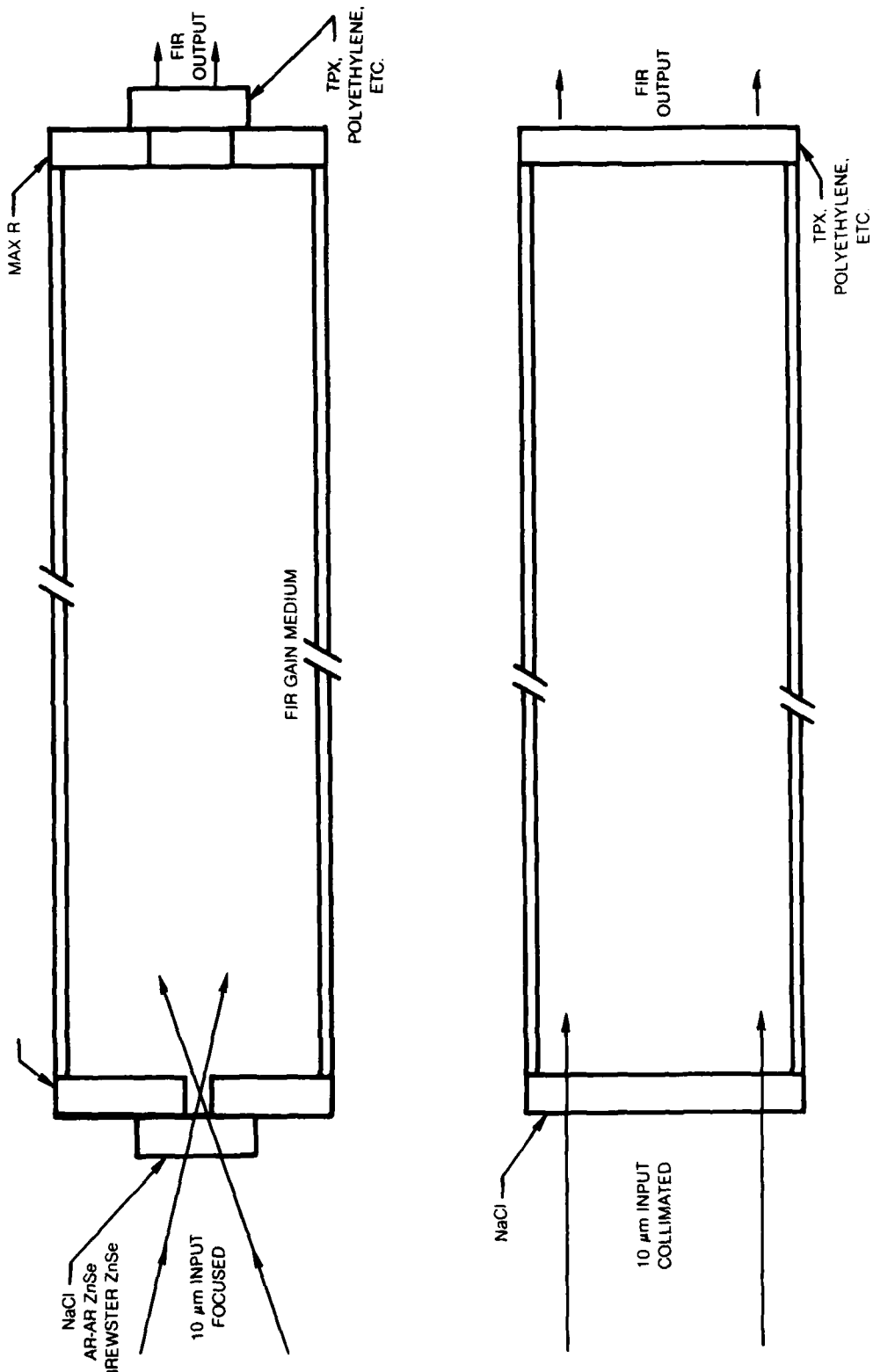

79–10–130–13

FIG. 15

ONE METER STEEL FIR GAIN CELL

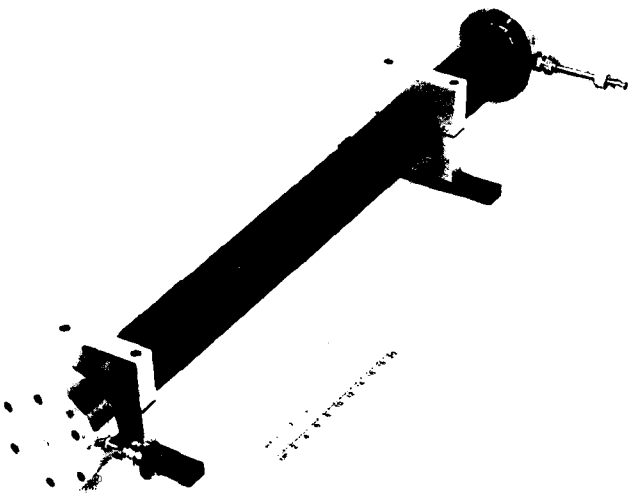

79–10–130–17

large aperture and small aperture output couples were used. Apparently as a consequence of the short gain length no FIR lasing was observed for any optical configuration tried. A second FIR gain tube 2.5 meter in length by 38 mm in diameter was therefore constructed (see Fig. 2) in the interest of bracketing the required FIR gain length for the available 100-150 mJ pump energy. With the 38 mm diameter the laser is expected to oscillate in a waveguide mode, and laser oscillation was obtained for several resonator geometries. When operated with a focused input beam the input spot size was adjusted to match a 6 mm diameter hole in the total reflector which served as the input mirror. This geometry is shown at the top of Fig. 14. The pump beam divergence in this configuration was such that the pump beam just matched the waveguide bore after one pass. At a PRF of 50 Hz with 5 w of 9.55 m power input the average FIR output power at 496 μm was .74 mw which corresponds to a power conversion efficiency of 1.4×10^{-4}. Average FIR power was measured with an Eppley thermopile which was approximately calibrated using a HeNe laser of known power. Most such detector surfaces are considerably more reflective at submillimeter wavelengths than in the visible and these FIR power measurements may be pessimistic by as much as 20-40 percent. Operating pressure was not critical in the 700 millitorr-1 torr range, but above 1 torr the FIR power begins to drop. At the optimum pressure approximately 70 percent of the input CO_2 radiation is absorbed by the gain medium. The fractional CO_2 absorption could be increase by using an even longer gain cell or by providing a shorter pump pulse so that a higher CH_3F pressure could be used without a commensurate increase in collisional dexcitation of the upper level. With CH_3F as the gain medium the power output is not notably sensitive to resonator configuration. Use of a collimated input beam as shown at the bottom of Fig. 14 gives approximately the same power output as the focused input case. Apparently the increased mode volume of the collimated input case compensates for the loss of feedback which occurs when the NaCl is substituted for the high reflectivity hole coupler. Similarly, addition of feedback at the FIR output coupler does not significantly affect FIR laser power.

In contrast to the methyl fluoride, methyl chloride (CH_3Cl) does snow a dependence of FIR output on pump frequency tuning and on FIR resonator configuration. The peak power of the 944 μm CH_3Cl line is maximum with the single mirror superradiant resonator (SSR) shown as the bottom illustration in Fig. 14, with the peak power being approximately 10-20 percent of the peak CH_3F power on the 496 μm line. The FIR output power is quite sensitive to the frequency of the TE CO_2 pump with the FIR oscillator falling below threshold for certain values of length tuning of the TE CO_2 pump. The use of a total reflector with 12 mm coupling hole as an output coupler reduces peak power by a factor of two from the maximum obtained with the SSR resonator, but the power stability is greatly improved, with fluctuation being on the order of ± 10 percent about the mean.

The optical pulse shape is of obvious importance for an FIR heterodyne system and significant differences were observed for the 944 μm line of CH_3Cl

and the 496μm line of CH_3F. Using the Schottky diode detector which will be discussed in more detail in a following section, the direct detected pulse shapes were determined for the 496 μm and 944 μm laser lines. Figure 16 shows the 496 μm line (or lines) of CH_3F. By comparing the pulse shape to the known pulse energy, we find an approximate peak power of 50-100 watts. Much structure is observed in this laser output when pumped by the 9.55 μm CO_2 wavelength. There are several rotational transitions (as many as 8) (Ref. 4) in the neighborhood of the principal 496 μm line and while the 100 mJ input beam does not represent a particularly high pump level, it is possible that more than one transition is above threshold. The presence of several longitudinal modes in the CO_2 pump output also presents the possibility of pumping several K levels within a given vibrational-rotational transition. Addition of a low pressure hybrid gain tube to the TE laser resonator can eliminate any longitudinal mode beating in the TE laser output, but it will not necessarily improve the tendency to oscillate on several different transitions. Figure 17 shows a typical 944 μm pulse from CH_3Cl. The reduced mode beating and absence of structure are noteworthy. This pulse tends to follow the CO_2 pump pulse, although the amplitude of the TE pulse tail is still insufficient to sustain 944 μm lasing above threshold.

The lower levels of typical optically pumped FIR laser transition have lifetimes which may extend into the millisecond range at the low pressures found in FIR lasers. As the PRF of a pulsed FIR laser is increased, the population dynamics will eventually converge to the equilibrium conditions of a CW FIR laser. This will be observed as a nonlinear increase of FIR power with PRF, and the transition region will be a function of gas pressure and gain cell diameter. We have measure average FIR power at 496 μm for PRF's from 50Hz to 350Hz and find no significant dependence of conversion efficiency on PRF over this range. Figure 18 summarizes the results of this measurement, showing the constancy of pulse energy.

3.3 CW Submillimeter Laser

The CW submillimeter laser serves as a local oscillator for heterodyne detection of target returns and may also be useful for injection controlling the pulsed submillimeter laser. CW FIR lasers have been operated with a variety of optical resonators including a conventional free-space mode resonators, waveguide resonators, and free space mode resonators in which the beam follows a zig-zag path through a gain medium which has a cross section greater than the beam cross section (Ref. 5). The waveguide resonator was chosen as most promising for the radar application as a result if its relatively high efficiency and compact size. The CO_2 pump beam is introduced into the FIR resonator by means of a small coupling hole, typical 3mm in diameter. The use of large coupling apertures as in the pulsed FIR resonator is not possible because of

FIG. 16

CH_3F PULSED OUTPUT AT 496 μm

SCHOTTKY DIODE DRIVING 50 Ω
VERTICAL: 200 mV/DIV
HORIZONTAL: 0.5 μs/DIV

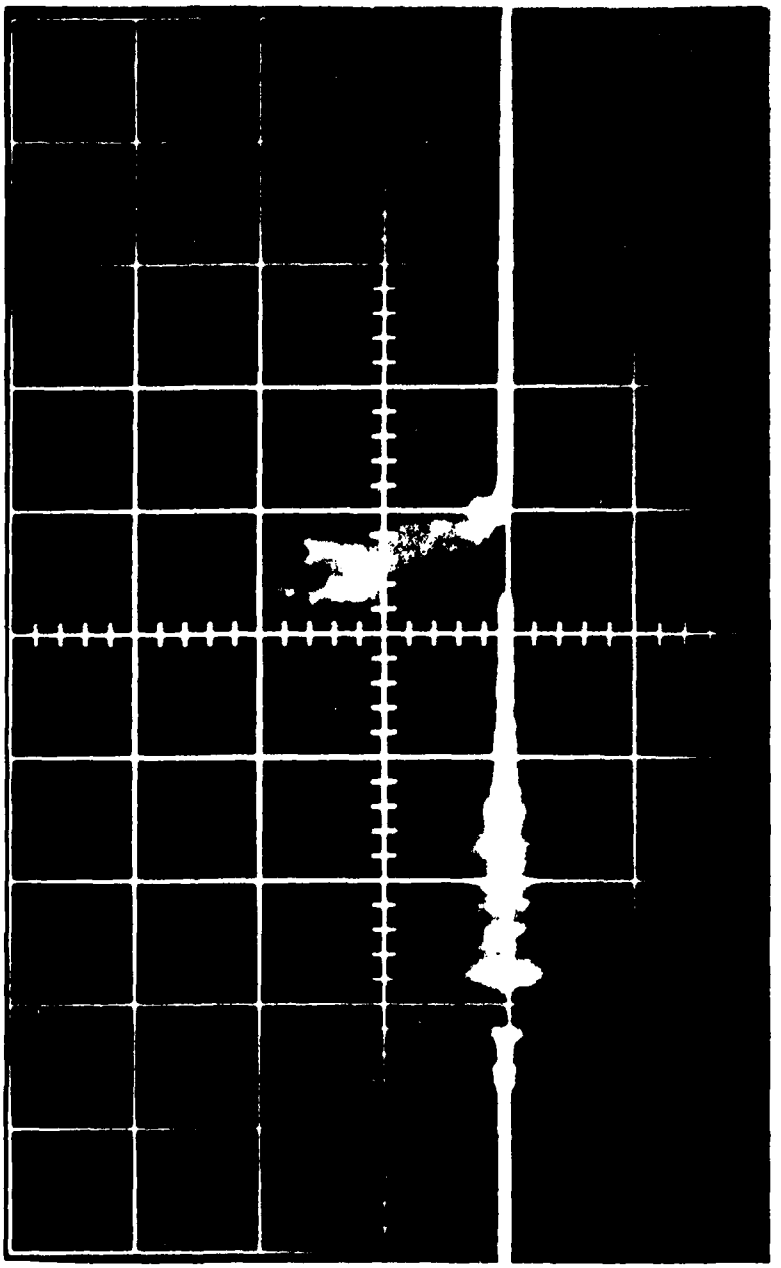

FIG. 17

CH_3Cl PULSED OUTPUT AT 944 μm

SCHOTTKY DIODE DRIVING 50Ω
VERTICAL 5mV/DIV
HORIZONTAL: 0.5 μs/DIV

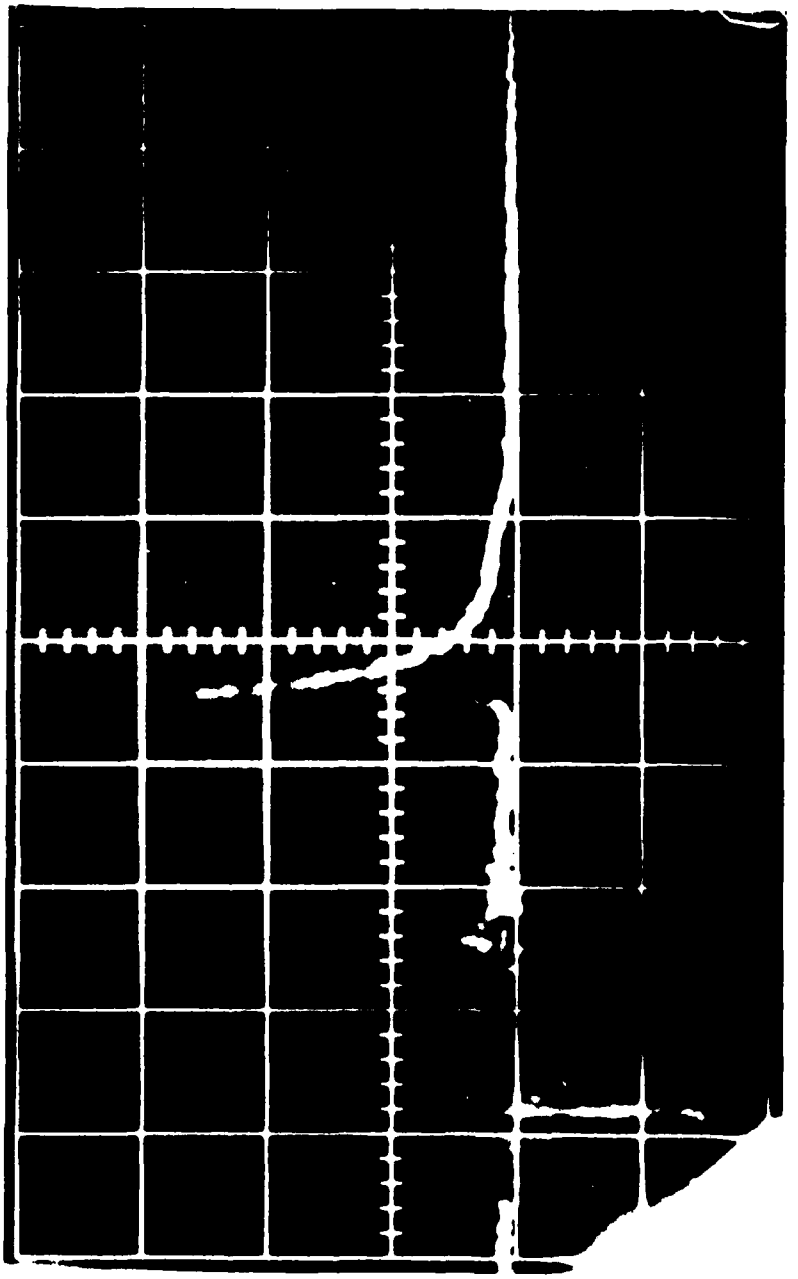

79-10-130-21

FIG. 18

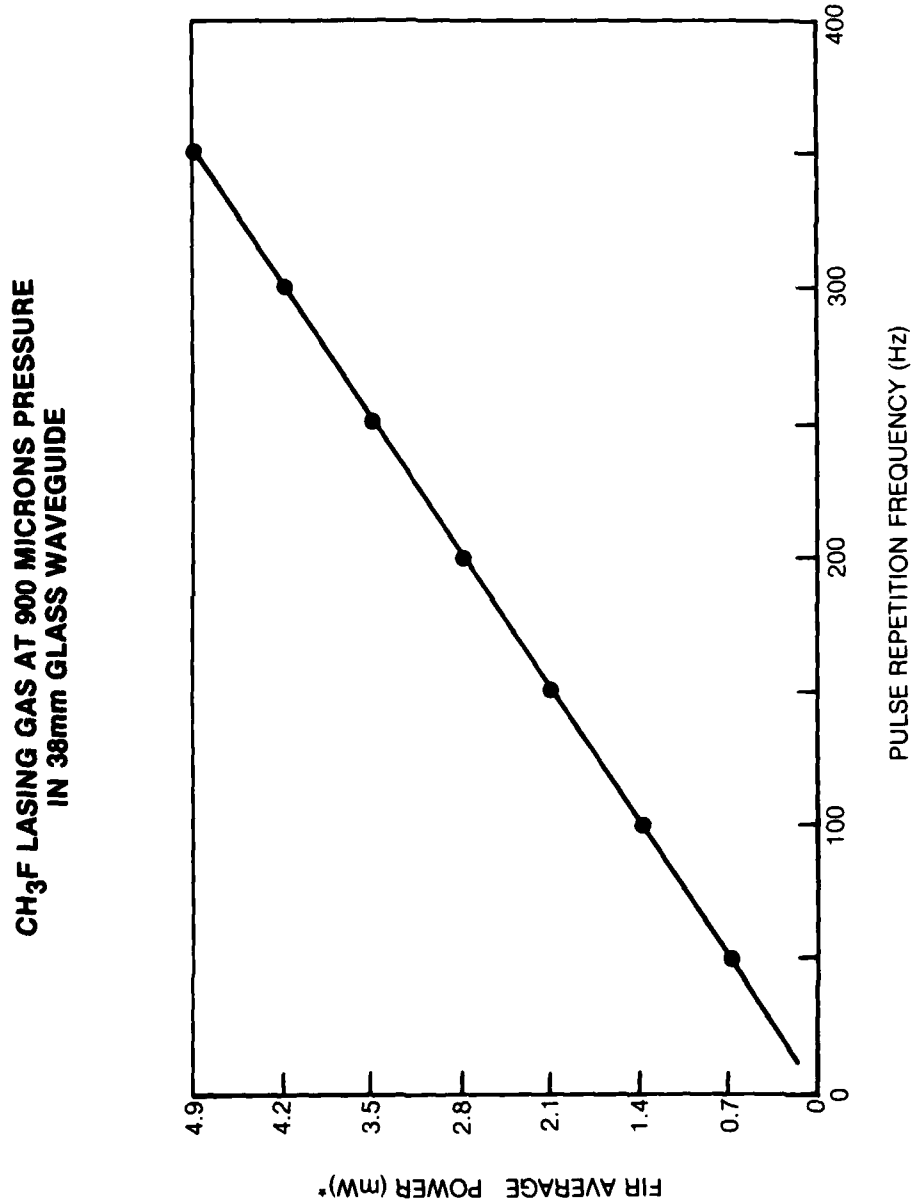

* POWER MEASURED WITH EPPLEY THERMOPILE. CALIBRATION IS APPROXIMATE AND MAY BE 20-40% BELOW ACTUAL POWER LEVEL.

79-10-130-14

the greatly reduced gain of the CW FIR laser. The unexcited FIR gain medium is capable of absorbing resonant submillimeter radiation and it is therefore desirable to have a uniform gain distribution parallel to the optic axis of the FIR laser. This uniform axial pumping may be effectively approximated by operating at a gain medium pressure which is low enough to permit multipassing the pump radiation in the FIR laser. The FIR resonator mirrors must therefore be highly reflective at the pump wavelength as well as at the submillimeter wavelength, in contrast to the pulsed submillimeter case. This is easily provided at the pump input end of the laser by using a fold coated mirror with a coupling hole. The FIR output coupler on the other hand must be a partial transmitter at the submillimeter wavelength and a good reflector at the pump wavelength. A mirror design which we have found satisfactory is illustrated in Figure 19. The high resistivity single crystal silicon substrate is first coated for high reflectivity over the 9-11 μm range of wavelength, and is then overcoated with gold except for a circular region (8-15 mm diameter) in the center of the mirror. The 10 m reflective coating is selected for high transmission at wavelength of interest (> 100 μm) and the silicon mirror is therefore effectively a hold coupler at submillimeter wavelengths. Standard silicon substrates were initially tried as FIR mirror substrates and although the absorption was acceptably low at the 119μm methanol line, there was no appreciable transmission at either 496 μm or 944 μm for any of five substrates tested. The 100L-cm silicon was found to have negligible absorption loss from 100 μm to 1000 μm. As in case of the substrate material a proper choice of coating materials was also found to be essential for proper laser operation. Based on 118 μm transmission measurements ZnSe-ThF_4 coatings were found to be very lossy while ZnS-Ge coating have negligible transmission loss (Ref. 6).

The complete cw FIR laser is shown in Figure 20. Overall laser length is 1.5 meters and the pyrex waveguide is 38 mm in diameter. The resonator is thermally stabilized with four invar rods and is made mechanically rigid by means of an L-shaped aluminum frame. The laser can be length tuned over a distance of 1 mm by means of a manually adjustable vacuum feedthrough on which the input beam hole coupler is mounted. This mount is shown in Figure 21. The input coupling structure uses an antireflection coated ZnSe window for vacuum seal. The FIR output end of the laser is shown at the bottom of Figure 21. Z-axis cut crystalline quartz is used as the vacuum seal at the end since it has excellent transmission over all wavelengths of interest. The cw FIR laser was designed to be operated in a sealed-off mode in order to make it feasible to use toxic gases such as CH_3Br and costly isotopic species such as $C^{13}H_3F$. A concession to overall vacuum integrity was made in using demountable optical elements, but the added freedom of being able to change resonator elements was deemed necessary for the current developmental program. The ultimate leak rate of laser is limited by the quality of the optical element seals, and using neoprene O-rings between lapped flange surfaces it was possible to achieve sufficiently low leak rates (2-3 millitorr per hour) to permit operation over an

FIR PARTIAL TRANSMITTER

- LASER OPTICAL ELEMENTS
  - Si HOLE COUPLER
    - STANDARD POLYCRYSTALLINE SI OPAQUE
    - 100Ω cm LOW LOSS
    - ZnSe-ThF_4 COATINGS VERY LOSSY
    - Ge-ZnS LOW LOSS

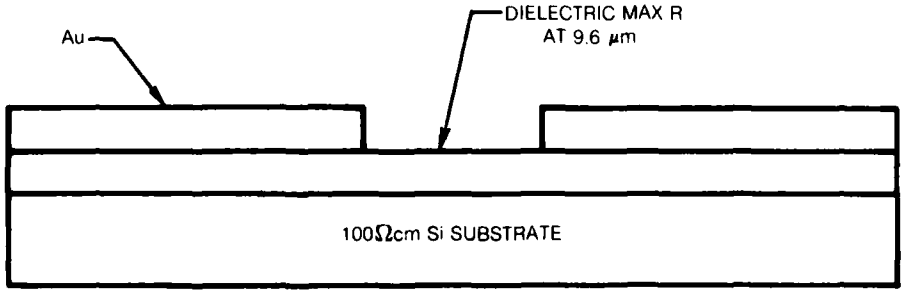

- CW POWER AT 496 μm
  - >5 mW MEASURED ON CALORIMETER
  - FOCUSED, CHOPPED ON SCHOTTKY DIODE

79–10–130–8

FIG. 20

CW FIR LASER

79-10-130-25

FIR MIRROR MOUNT ASSEMBLY

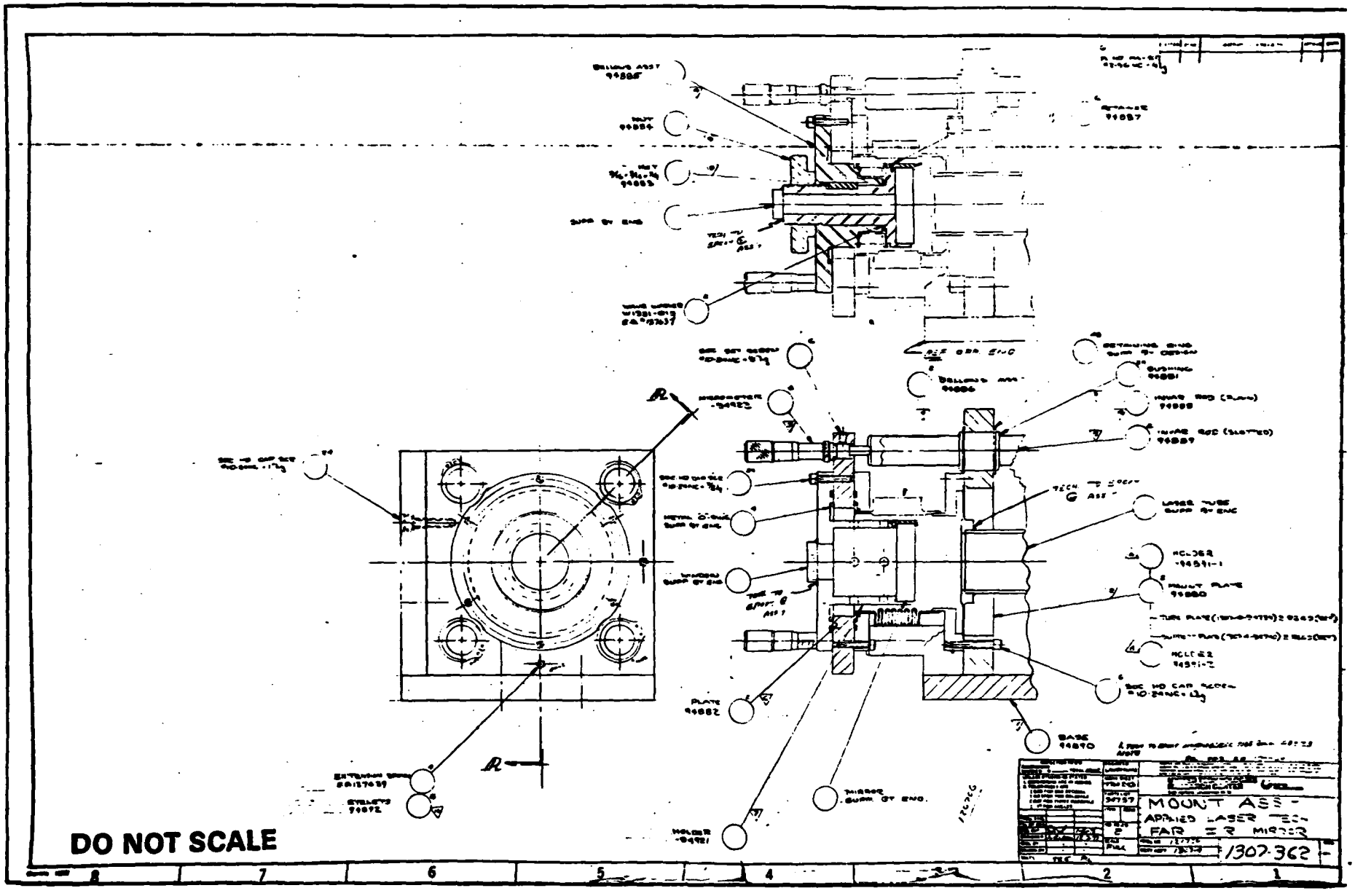

eight hour period with a single gas fill. For truly long-term sealed operation a higher quality vacuum seal will be needed. Hollow, silver-plated stainless steel O-rings were tried as laser vacuum seals but leak rates were unacceptably high even with highly polished flange surfaces. Indium wire seals formed by fitting a 1/8" indium were into the O-ring groove and overlapping the two ends of the wire have also been investigated, and these appear to offer the best long-term sealing characteristics. However, these seals were not included in the delivered hardware because they are not reusable and a certain amount of technique must be learned before one can be resonably certain of getting a high vacuum seal. Because epoxy seals were used at several joints in the laser built for this program the assembled lasers could not be outgassed at temperatures above approximately 130°F. The pressure response of the system to heating indicated that temperatures higher than 120°F would have further improved the base pressure of the system. A long life system should therefore incorporate glass-metal seals which permit welding or brazing the optical mounts to the waveguide rather than using epoxy for this purpose.

Because of the mechanical complications associated with intravacuum optics and the low operating pressure ($\sim$ 100 millitorr), the vacuum integrity and sealed lifetime of the cw FIR gain cell remain as technical issues that are not fully resolved.

The gain length of 120 cm chosen for the cw FIR lasers is relatively short and was selected in the interest of parameterizing the more compact lasers for which little data are available in the literature. The submillimeter output power was found to be sensitive to input beam probe matching and two mode matching configurations are presented in Figure 22. The optical configuration of Figure 22a produced a theoretical spot size of .9 mm at the 3 mm input coupling hole of the FIR laser and this focussed spot size was achieved to within 10% using the cw CO_2 laser which will be described in Section 3.4. For the 496 μm line of CH_3F using 25 watts of 9.55 μm pump power a maximum output power of 7mW is obtained at the optimum pressure at 75 millitorr. Using the mode matching configuration of Figure 22b the spot size is reduced by 25%. The primary effect of the stronger focus is to increase the divergence of the pump beam within the submillimeter laser resonator. Although the increase in divergence is relatively small, the optimum pressure falls to approximately 40 millitorr and the maximum power decreases to approximately 4.5 mW for the same pump power. This trend suggests that perhaps an input spot size larger than .9 mm should be used, however this will require an input coupling hole large than 3 mm in diameter and two undesirable pheromena occur as the input hole size is increased. First, as the input beam is matched to larger hole sizes the divergence of the pump beam decreases and an increasingly large fraction of the pump beam escapes from the FIR resonator after one round trip. This reduces efficiency and contributes to instability of the pump laser since the retroflected beam is coupled back into the pump laser. The second effect is the obvious

FIG. 22

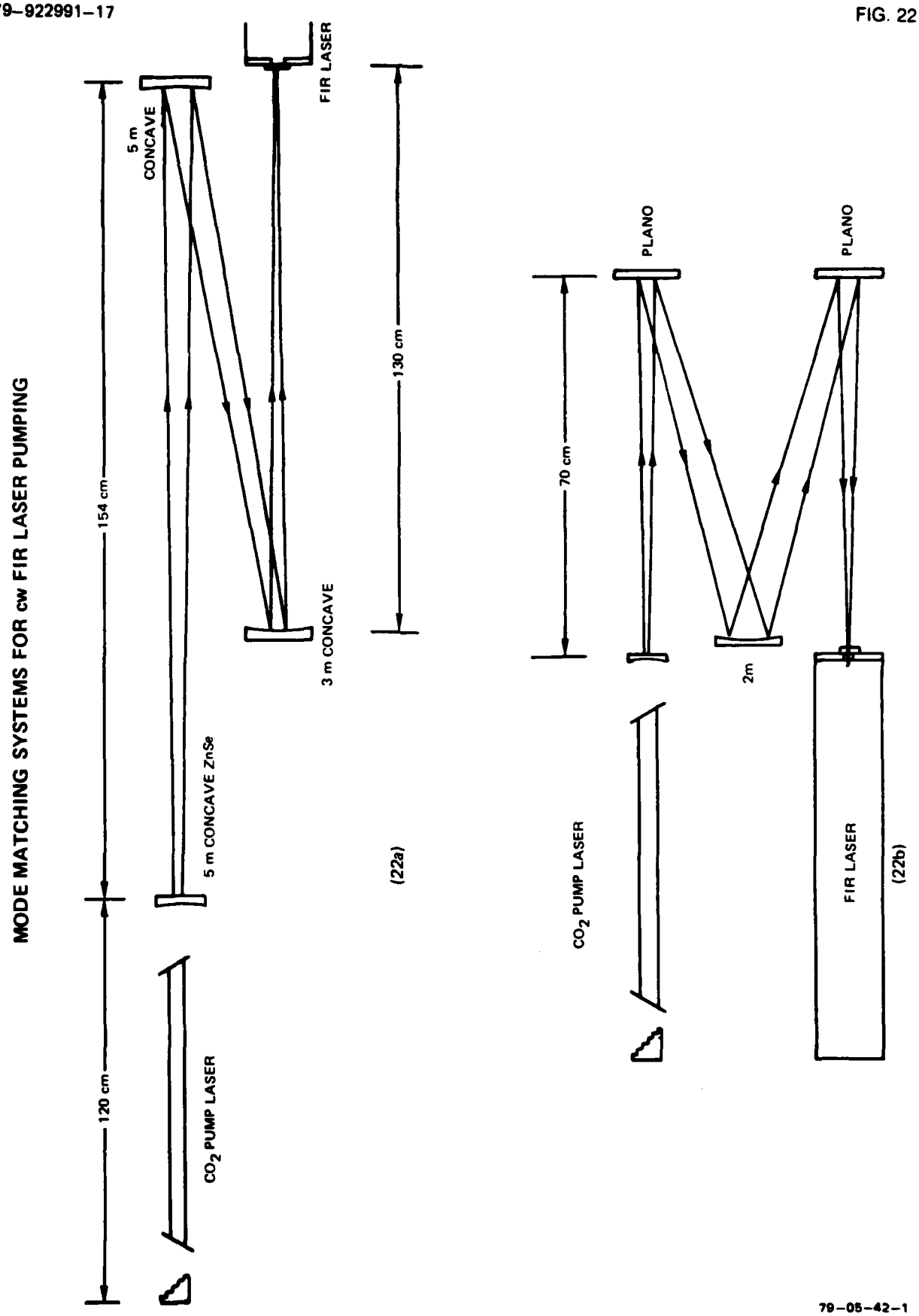
MODE MATCHING SYSTEMS FOR cw FIR LASER PUMPING
5 m CONCAVE
FIR LASER
154 cm
130 cm
3 m CONCAVE
5 m CONCAVE ZnSe
120 cm
CO_2 PUMP LASER
(22a)
PLANO
PLANO
70 cm
2m
CO_2 PUMP LASER
FIR LASER
(22b)
79-05-42-1

increase in FIR cavity loss that results from the input aperture which reduces laser power not only by increasing loss but also by tending to support oscillation in an annular mode which is less effectively coupled from the intended output coupling aperture. Laser power was measured with Scientech Model 360001 power meter which has a reduced sensitivity at FIR wavelengths as a result of the increased reflectivity of the sensor surface at the long wavelengths. Power readings may underestimate the power by as much as 40% though this appears to be an outside limit.

The optical coupling of the FIR and CO_2 pump resonators results in a long warm-up time before FIR laser output stabilizes. The FIR cavity length tunes as a result of the CO_2 pump heating, and the drifting phase of the pump radiation that is reflected back into the CO_2 resonator causes the CO_2 pump frequency to drift. The change of CO_2 frequency produces a changing thermal input to the coupled resonator system and the resulting dynamic behavior of the coupled system can have a very complex temporal history. It is possible that for certain system parameters the FIR output power could be oscillatory in time, although we generally observed long-term warm-up times on the order of two hours for the passively stabilized system. The need for active control of both CO_2 and FIR lasers is clear for this coupled resonator system and since thermal effects are dominant a control bandwidth of 10 Hz or even less should greatly improve laser stability.

3.4 CW CO_2 Pump Laser

The operational characteristics of the cw submillimeter are strongly dependent on the quality of the CO_2 pump laser. The design goals and performance characteristics of the cw CO_2 pump laser are listed in Figure 23. Like the submillimeter laser resonator, the CO_2 laser is thermally stabilized by Invar rods and is mechanically rigidized by an L-shaped aluminum framework. This laser is shown in Figure 24. The laser has a one meter gain length and a 1.2 meter resonator. Laser power is dependent on gas mixture and flow rate and for slow flow (less than 1 cfm) a maximum power of 54 watts is obtained using a 5 meter concave output coupler with 25% transmission and a flat total reflector. Use of a Littrow grating end reflector is necessary for rotational line control and a loss of 7-20 watts in output power is typical depending on grating quality. Using a high quality grating on a metal substrate (Ref. 7), 47 watts can be obtained on the 10P(20) line, whereas the more resilient original rulings are typically more variable in quality and the range of powers obtained with original rulings span the range of 44 watts to 30 watts. Ideally one would like to be able to tune the CO_2 laser over a complete free spectral range without switching from the TEM_{oo} mode, assuming that TEM_{oo} output is achievable. If the CO_2 laser is free, or nearly free, of transverse mode switching, the stabilization logic can be much simpler than if mode beating noise is present and the power tuning curve has multiple maxima within one free spectral range. Unambiguous TEM_{oo} operation is desirable even in the absence of control loops since the higher order modes have had different focusing characteristics and generally coupled to the FIR resonator less

FIG. 23

CW CO_2 PUMP LASER

- REQUIREMENTS
  - POWER, >20 WATTS
  - MODE, TEM_{00} FOR LARGE f-NUMBER, SMALL INJECTION HOLE
  - GRATING CONTROLLED
  - FREQUENCY STABLE, NARROW FIR ABSORPTION LINE
    ALSO IMPLIES TEM_{00}
- PERFORMANCE
  - 30-40 WATTS TEM_{00} IN 9P20
    FUNCTION OF GRATING QUALITY
  - THERMAL LOADING OF GRATING AND BREWSTER WINDOWS GREATLY IMPACTS FREQUENCY
    STABILITY AND TRANSVERSE MODE PURITY
    WATER COOL GRATING AND WINDOWS
  - DIFFRACTION LIMITED PERFORMANCE WITH f/100 FOCUSING OPTICS ACHIEVED
    SUBSTANTIALLY DEGRADED BY LOSSY OR DISTORTED OPTICAL ELEMENTS
  - CAREFUL MODE-MATCHING INTO INJECTION HOLE REQUIRED
    USE OF STANDARD OPTICAL ELEMENTS SIGNIFICANTLY LENGTHENS OPTICAL TRAIN

79-10-130-1

FIG. 24

50 WATT CW CO_2 LASER

79 10 130 22

efficiently than the TEM_{oo} mode. We have found, for example, that whereas a certain mode matching configuration may couple 95% of the TEM_{oo} power into the FIR resonator, this same system couples only 65 percent of the next higher mode into the same FIR resonator.

Obtaining reliable and efficient, TEM_{oo} operation in higher power CO_2 lasers can be quite difficult due to the tendency of "whisper modes" to oscillate in the high gain regions of the plasma near the glass walls. One can formulate a CO_2 laser design approach which is based on increasing the differential loss between the TEM_{oo} and TEM_{10} modes by using one or two apertures at either end of the laser (Reference 8). This approach has not, in our experience, proven adequate for the higher power CO_2 laser because it ignores the influence of the plasma bore as a guiding surface for the troublesome whisper modes which can dominate the laser output. In the course of the current program it was established that the higher order modes could be effectively suppressed by providing several constrictions spaced 15-20 cm apart inside the plasma tube. Initially the constriction were formed directly into the 9mm I.D. plasma tube by indenting the glass at several places to form an 8mm aperture. An equally effective method, and one which is much simpler to implement is to use several Invar rings which fit the 9mm tube I.D. and have a .4mm wall thickness. The rings are split to provide some flexibility and are simply slipped into position in the plasma bore. Both of these aperturing systems have been found to yield reliable single mode laser operation with no significant (less than 5 percent) reduction in the unapertured laser power. The tuning range over which TEM_{oo} operation occurs is a function of gas mixture and tube current. When current and/or mix are adjusted to yield a high saturation power and lower unsaturated gain the laser may actually be turned off by length tuning. When higher gain mixes or low tube currents are used transverse mode switching may occur at as much as 75 percent of line center power. The lower gain mixes which typically require higher currents and provide the best transverse mode discrimination yield the same power as higher gain condition, but laser efficiency may be reduced to 9-10 percent which is still acceptable for a single mode laser.

A final consideration in maintaining a single mode output is the need to cool intracavity optical elements. Brewster windows were determined to be a major source of instability until water cooling was provided at each window. The Littrow grating also requires water cooling to reduce its susceptibility to damage and to reduce the long term thermal drifting which occurs when the grating must come to equilibrium at temperatures well above room temperature.

As in the case of the pulsed TE_{oo} CO_2 pump source, the cw CO_2 pump laser is a major component of the radar system, having a significant impact on size, reliability and power consumption. Operating the laser in a Q-switched mode would reduce its size but the impact on mode purity and frequency stability is uncertain at present.

3.5 Submillimeter Wave Detectors

A pulsed heterodyning submillimeter was radar will require a high efficiency detector with 5-50 MHz bandwidth. The semiconductor photon detectors, GaAs in-particular, are very sensitive but response falls off quickly above 1-2 MHz and cooling to liquid helium temperature is required. The Schottky diode appears to be the best choice for a wideband sensitive detector at submillimeter wavelengths and the bulk of detector work within the current program has been concentrated on this type of detector. Pyroelectric detectors were for a time considered for use as laboratory pulse detectors and potentially as high signal level heterodyne detectors. Fast pyroelectrics with response times on the order of one nanosecond have become available in recent years and they appeared to offer the possibility of a fast and rugged if somewhat insensitive FIR detector. Two commercially available high speed pyroelectric devices were investigated (Reference 9) and although both detectors functioned satisfactorily in detecting pulses faster than 100 ns, they exhibited severe acoustic resonances when driven with pulses in the 300ns-3μs range. Figure 25 shows a typical pulsed output from a fast pyroelectric detector. The risetime is fast but the fall time and subsequent decay time are limited by the acoustic response of the detector and its substrate. This characteristic does not invalidate their use as pulse energy monitors once they have been calibrated; however we were always able to operate at a sufficiently high pulse rate that an average power reading could be used to infer pulse energy.

Schottky diode devices have been widely used as microwave detectors for many years, however devices with response into the 300-600 GHz range are not yet readily available and we therefore obtained a number of high quality diodes on a research basis from Dr. Robert Mattauch who has been developing these devices at the University of Virginia (Reference 10). Future references to Schottky diodes will refer exclusively to data obtained with University of Virginia devices. It should be also be noted that efficiently coupling submillimeter radiation to a diode detector remains a largely unsolved problem and any performance data must be considered lower limits which may considerably underestimate intrinsic device performance.

Figure 26 illustrates in cross section the construction of a Schottky diode. This structure bears a superficial resemblance to the point contact diodes which are commonly used as microwave detectors, but unlike the point contact devices the Schottky diodes utilize the one mil whisker only as an antenna and an electrical contact. The diode itself is formed by photolithography and does not depend on a tenuous contact with the pointed whisker. Figure 27 shows a detector chip which contains several hundred diodes (two small to be seen in this photo) and the phosphor bronze antenna wire which has been contacted to a single diode. The bend in the antenna wire defines the effective length of the antenna, thereby determining the antenna pattern (Reference 11); this bend is also needed to provide some spring force to maintain contact in the presence of ambient temperature variations.

FIG. 25

FAST PYROELECTRIC DETECTOR RESPONSE TO TEA CO_2 LASER OPTICAL PULSE

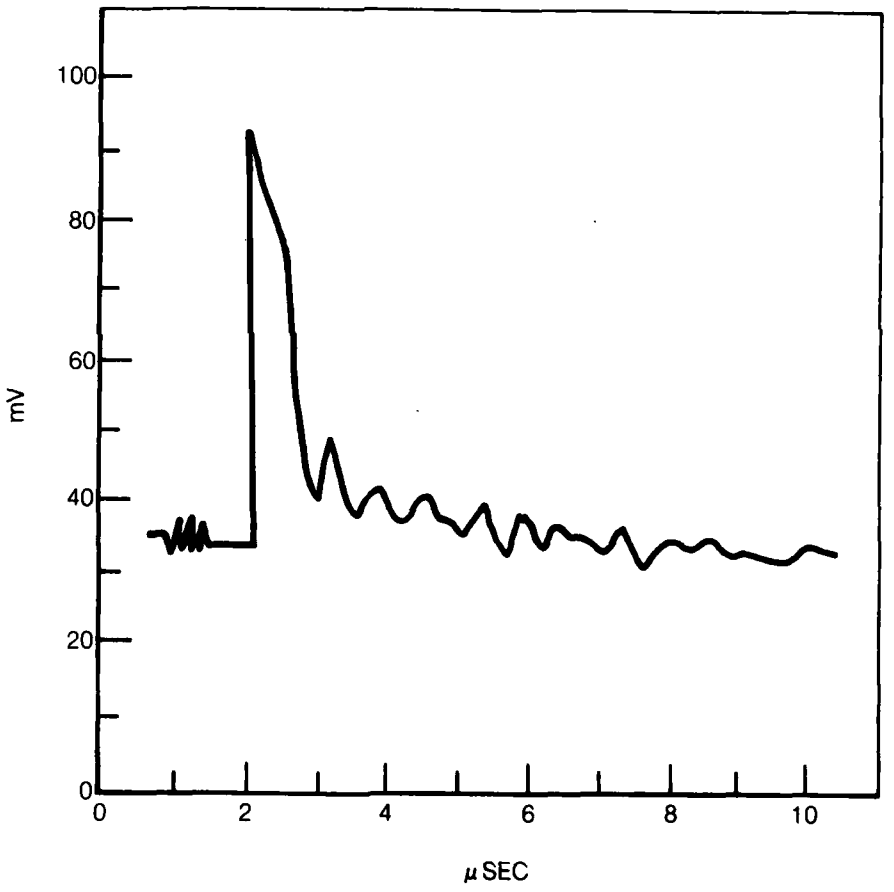

79-10-130-2

FIG. 26

DETAIL OF SCHOTTKY DIODE CONSTRUCTION

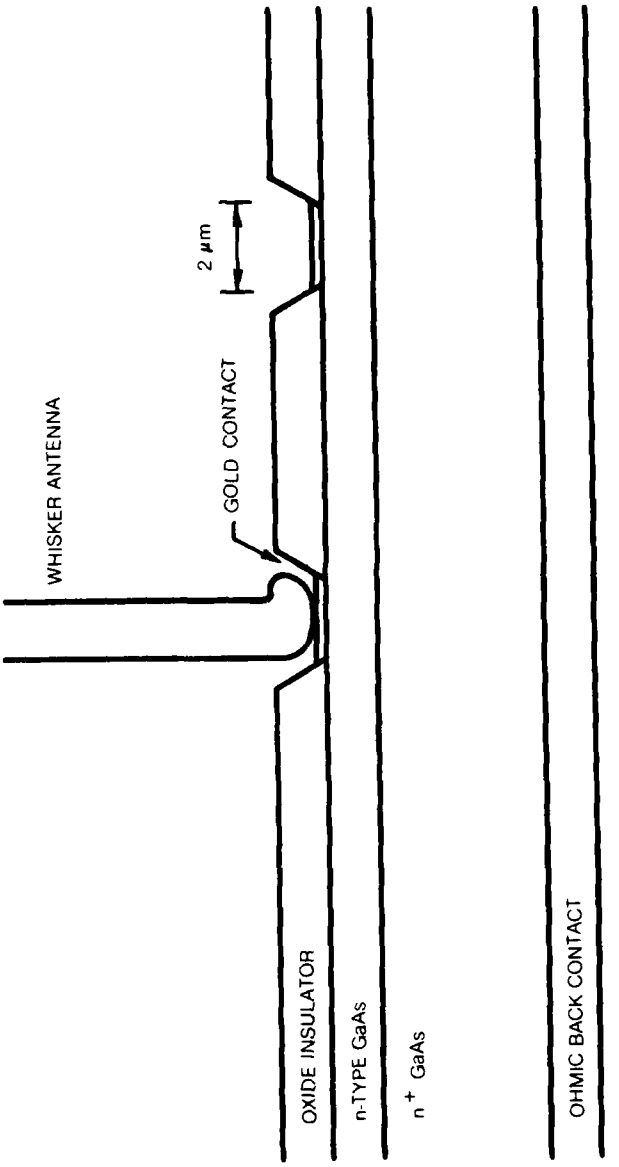

79-10-130-3

FIG 27

SCHOTTKY DIODE

MOUNTING POST IS 0.032 in DIAMETER

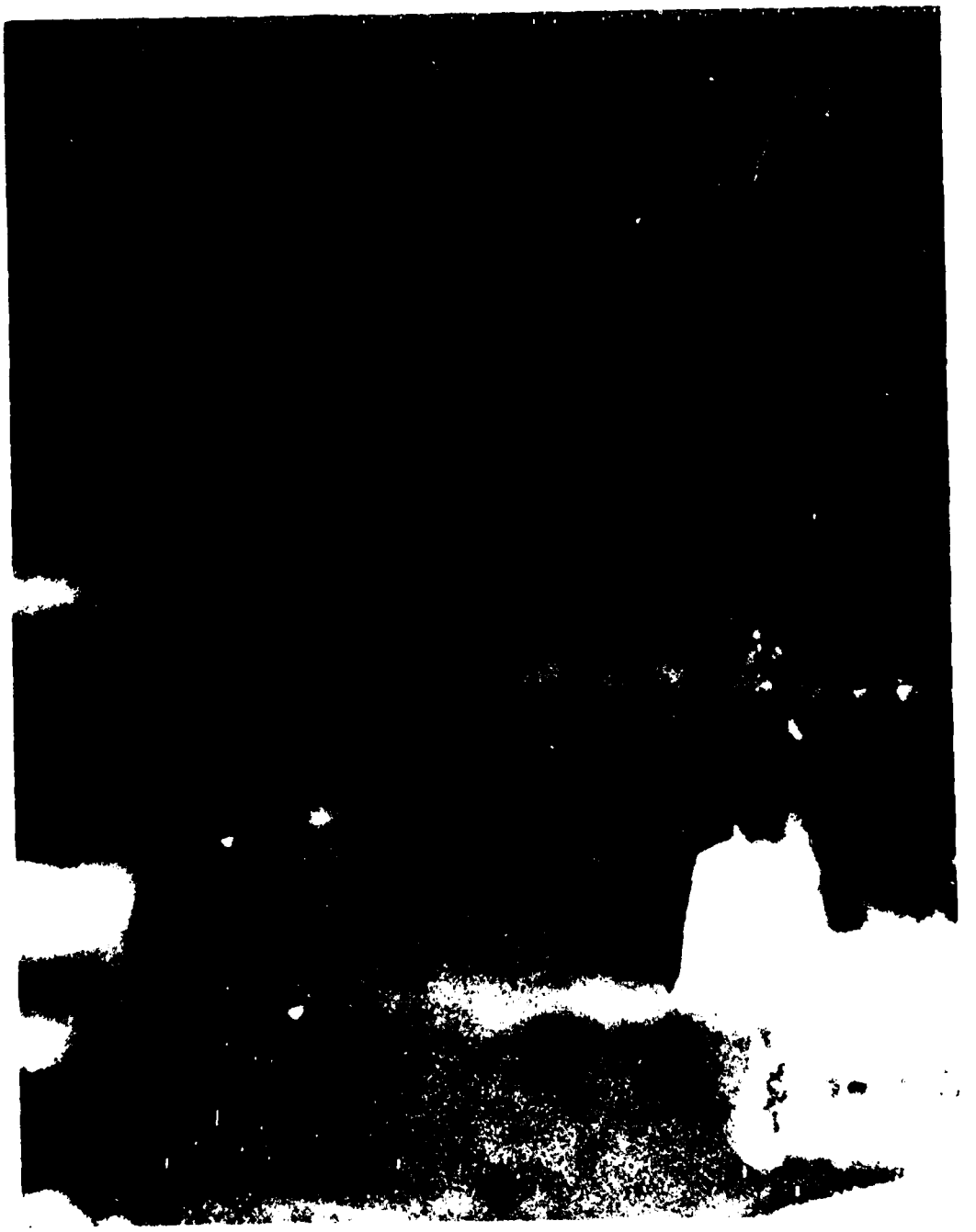

Of fundamental importance to the implementation of a heterodyning submillimeter detector is the signal-to-noise ratio obtainable with available local oscillator drive power. The maximum heterodyne S/N is obtained when local oscillator induced shot noise is the dominant source of detector noise; however if detector responsivity at the wavelength of interest is too low, shot noise limited operation may not be possible with available local oscillator drive power or the required drivepower may exceed the detector damage threshold. Using the output of the pulsed FIR laser it was established that the two micron diodes had a voltage responsivity of approximately 100mV/mW when terminated in 50Ω. In order to make a quantitative determination of diode response at local oscillator signal levels, the power from a cw 500μm laser was focused onto the Schottky using a 50 mm focal length paraboloidal mirror. The experimental arrangement is shown schematically in Figure 28. Because of the long wavelength and the 1 cm beam diameter at the focusing mirror, the focused spot size is expected to be several millimeters in diameter; consequently only a small fraction ($\wp$ .6%) of optical power is coupled to the detector. The signal passing through the detector structure was retroreflected by a 30 cm radius mirror with a resulting increase of approximately 30 percent in signal strength. The detector output was then amplified with a total voltage gain of 200, and the signal was viewed on an oscilloscope. Due to the lack of dc response in the amplifiers or a suitable 500 μm source with which to heterodyne, the detector signal was modulated by mechanically chopping the FIR laser output. The chopped waveform as viewed on the Schottky diode is shown in Figure 29. The irregular waveform is a result of the sizes of the beam and chopper aperture and and does not markedly affect the accuracy of the measurement. Considering the detector to have an effective cross section of $\lambda \times \lambda/2$, we find a detector response of 20mV/mW with 30 μamps of detector bias current. Currents less than 20 μamps result in no detectable response and increased bias currents do not increase detector output. The agreement between the pulsed and cw data reflects the considerable uncertainties in the measurement process which include: greatly differing signal strengths; uncertain beam profile in the focal plane of the collection optics; use of different diodes although electrical characteristics are expected to be similar. These measurements do clearly indicate the suitability of 2 micron Schottky diodes as room temperature detectors for wavelengths at least as short as 500μm, and the voltage sensitivity is comparable to that found in high quality microwave diodes.

For use as a submillimeter heterodyne detector, the simple optical mixer does not appear suitable because of the small fraction of local oscillator power which actually couples to the diode. The current experiments had a very high signal-to-noise ratio because the detection bandwidth was limited to 30 KHz; but if the detection bandwidth were increased to 10 MHz, as would more nearly be the case for the pulsed radar, the S/N will decrease to a value of two. The detector circuit used in the present work has been designed more for noise immunity than for ultimate responsivity and the noise (with or without power on the detector) is about five times the Johnson noise of the 50 Ω source impedance. It therefore

FIG. 28

CHARACTERIZATION OF SCHOTTKY DIODE AT MILIWATT SIGNAL LEVEL

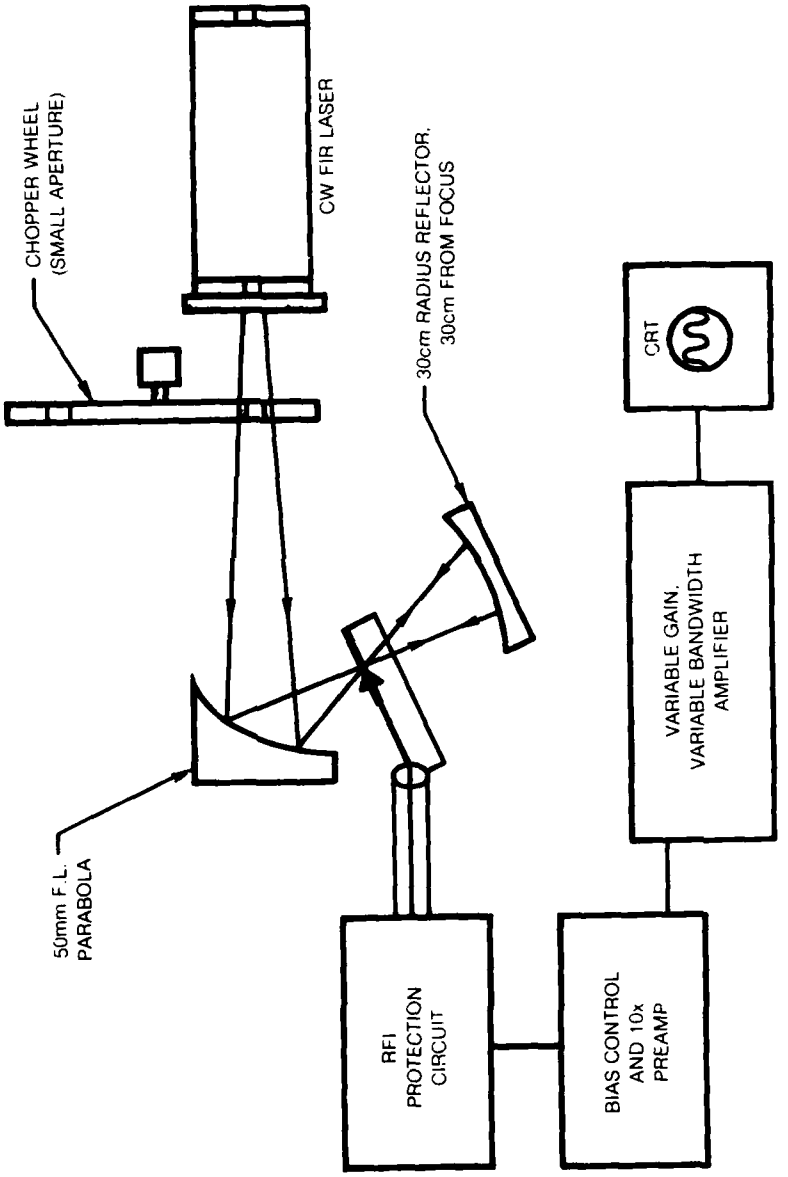

79–10–130–4

FIG. 29

CHOPPED CW 496 μm LASER OUTPUT-2 mW AVERAGE POWER

200x VOLTAGE GAIN. 30 KHz BANDWIDTH
VERTICAL: 5 mV/DIV
HORIZONTAL: 0.5 MS/DIV

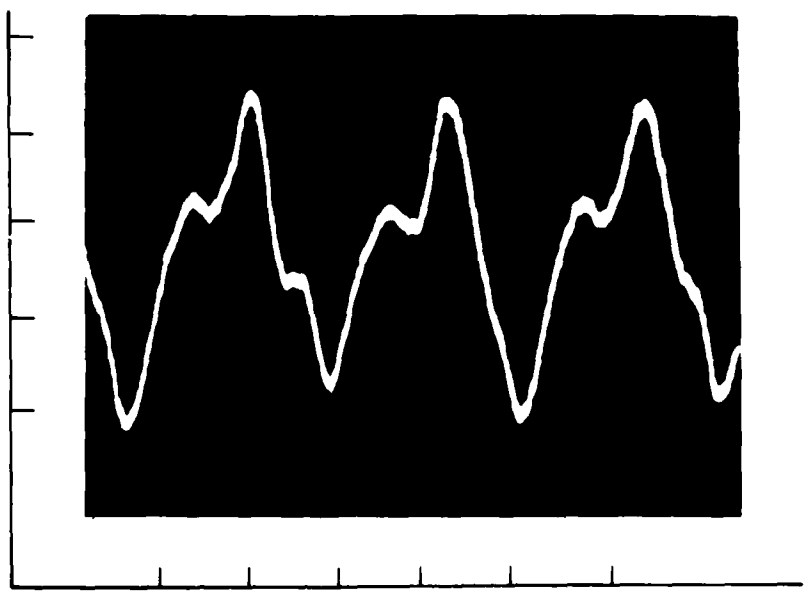

79–10–130–18

appears that while some gain in S/N may be realized by further reducing detector circuit noise, the greatest dividends will result from improving the coupling of the submillimeter radiation to the detector and possibly increasing local oscillator power, although the latter is probably not necessary if efficient coupling is achieved. Figure 30 summarizes the performance of the Schottky detector in the RFI protected circuit discussed below. In order to investigate waveguide coupling techniques, waveguide components suitable for 325 GHz operation were ordered midway through the program. Although the ordered waveguides and couplings were readily available in principle, the components were never delivered and no satisfactory explanation was ever received. This experience was not totally unexpected and is symptomatic of the generally limited development of the submillimeter wave technology.

3.5.1 Schottky Detector Modules

In the course of the detector experiments it was found that the RFI from the TEA Co_2 laser was of sufficient magnitude to destroy an unshielded Schottky diode and it was therefore necessary to install the diode is an RFI shielded module. Two detector modules were built for delivery under this contract for use as wideband pulse detectors or for detection of modulated cw laser output. Figure 31 shows the assembled detector module mounted on a fixed stage with a 50mm focal length parabolic collection mirror. The collection mirror is attached to a two-axis optical mount to facilitate beam alignment onto the detector. Figure 32 shows the detector module with RFI shielding tubes which we have found useful when working in close proximity to the TEA laser. For effective RFI shielding it is necessary that the tubes be a few inches longer, and this precludes the use of the low $f^{\#}$ collection optics; however, when working close to the TEA laser signal strength is not normally a problem. Unfortunately the damage potential of a given RFI source is very difficult to predict and the conservative approach would be to use the shielding tubes whenever the focusing mirror is not needed to obtain sufficient signal intensity. Even without the shielding tubes the detector is well protected from the ground loop voltages which can be the major source of noise currents. As a very rough reference point, we have had no problem in using the detector without shielding tubes at a distance of two meters from the TEA laser. The optical damage threshold for the detector is best stated in terms of the detector current. 10 ma is an upper limit and should not be sustained for more than a minute or so; 5 ma and less are safe current levels for continuous operation. Figure 33 shows the internal structure of the detector-preamplifier assembly with the RFI shielding removed. Figure 34 gives detector mounting details. In the event that the detector should need to be replaced, the entire brass mount is removed by releasing the mounting screws. Electrical contact to the pin on which the diode is mounted is by means of silver conductive paint which may be dissolved with acetone. A rechargeable Gates cell provides power for the Avantek amplifier

FIG. 30

SCHOTTKY DETECTOR PERFORMANCE IN RFI PROTECTED CIRCUIT

- VOLTAGE GAIN: 200x @ 50Ω OUTPUT IMPEDANCE
- SIGNAL LEVEL: 20mV FOR 2mW FIR POWER (TWO-PASS) AND 30μ AMP BIAS
- NOISE LEVEL: 150μ V FOR 30KHz BANDWIDTH
- EXPECTED NOISE FOR 10MHz BANDWIDTH: 9mV
- EXPECTED SIGNAL-TO-NOISE RATIO FOR 10MHz: ~2
- ROOM TEMPERATURE JOHNSON NOISE FOR 50Ω : 0.16μ V x 200 = 32μ V

- RECOMMENDATIONS:
  - INCREASE LOCAL OSCILLATOR DRIVE POWER
  - MINIMIZE NOISE SOURCES IN RFI PROTECTION CIRCUIT
  - IMPROVE DETECTOR CONVERSION EFFICIENCY BY IMPROVING OPTICAL COUPLING TO DIODE

79–10–130–5

FIG. 31

SCHOTTKY DETECTOR PACKAGE WITH PARABOLIC COLLECTION MIRROR

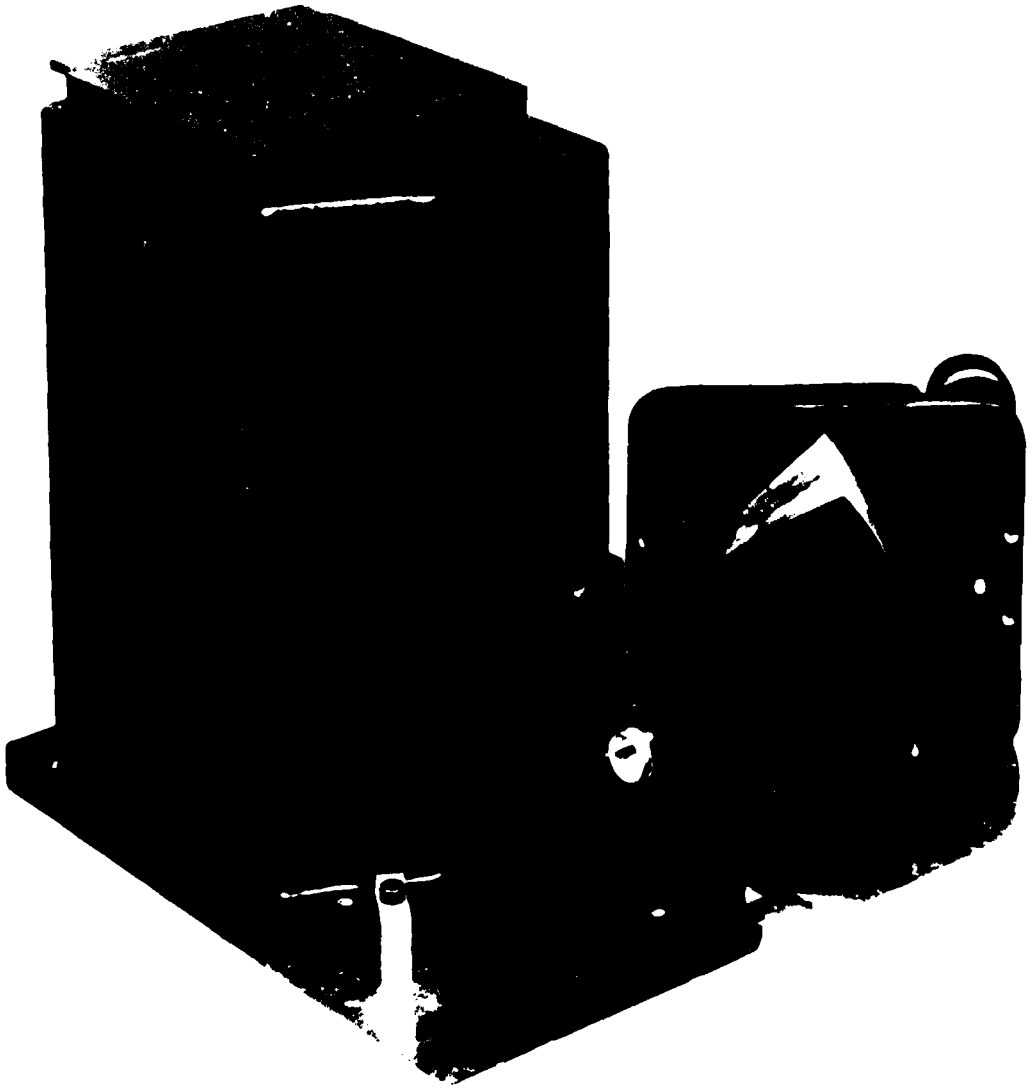

FIG. 32

SCHOTTKY DETECTOR WITH RFI SHIELDING TUBES

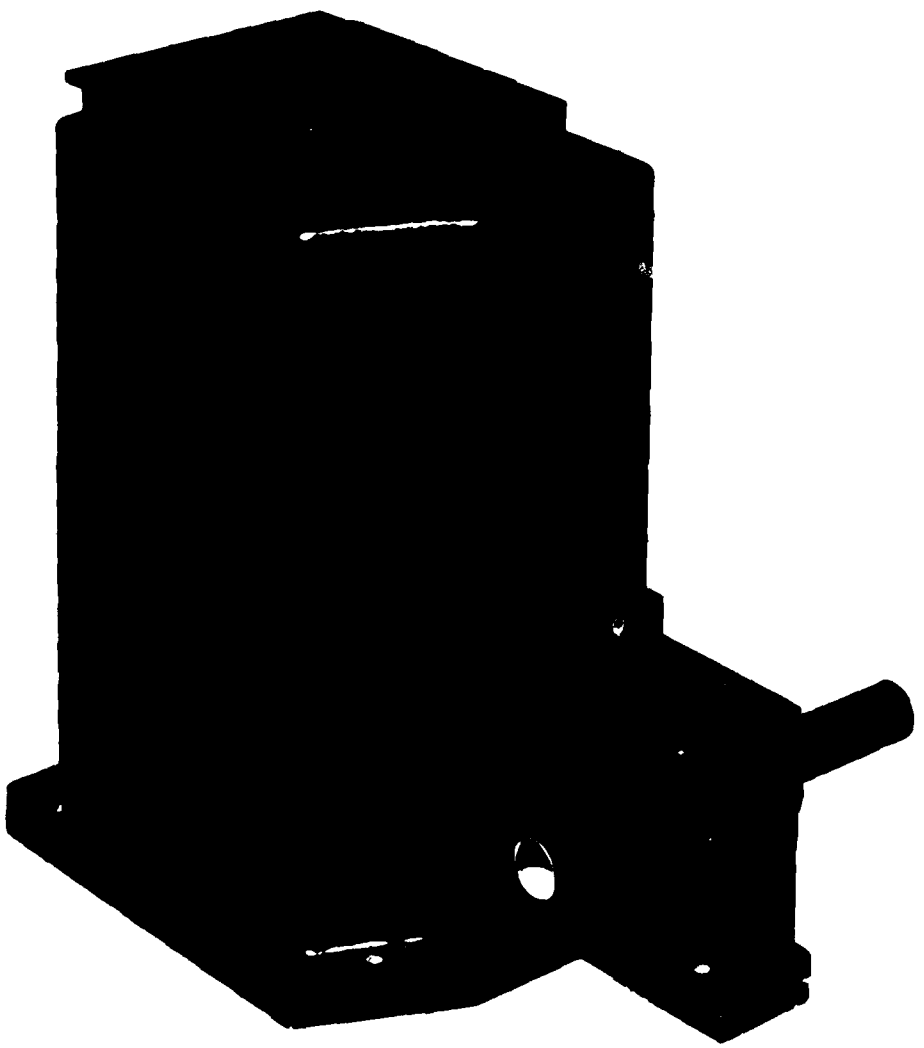

FIG. 33

ASSEMBLY VIEW OF SCHOTTKY DETECTOR SHOWING WIDEBAND AMPLIFIER

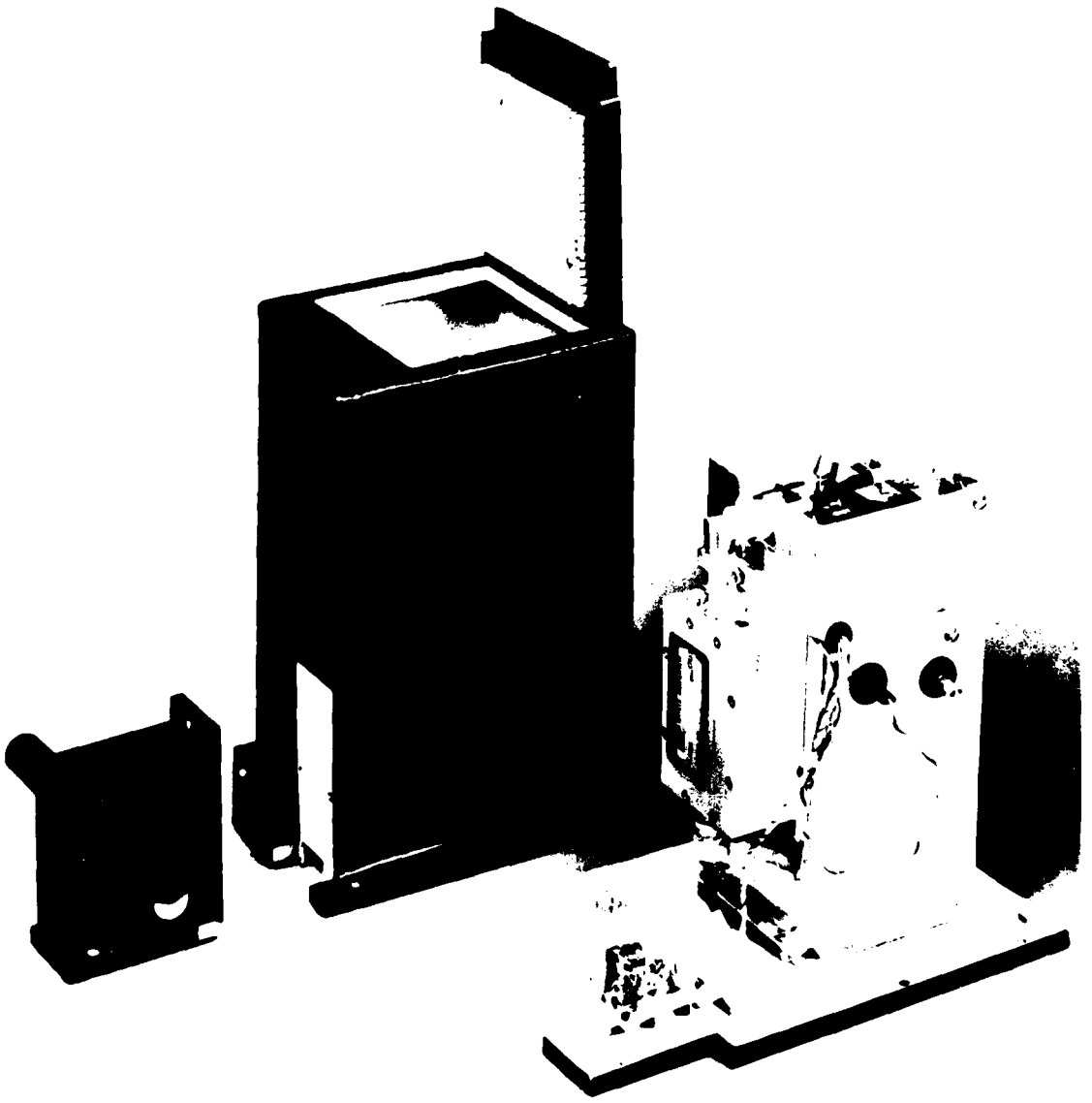

DETAIL OF DETECTOR HEAD SHOWING SCHOTTKY DIODE IN BRASS MOUNT

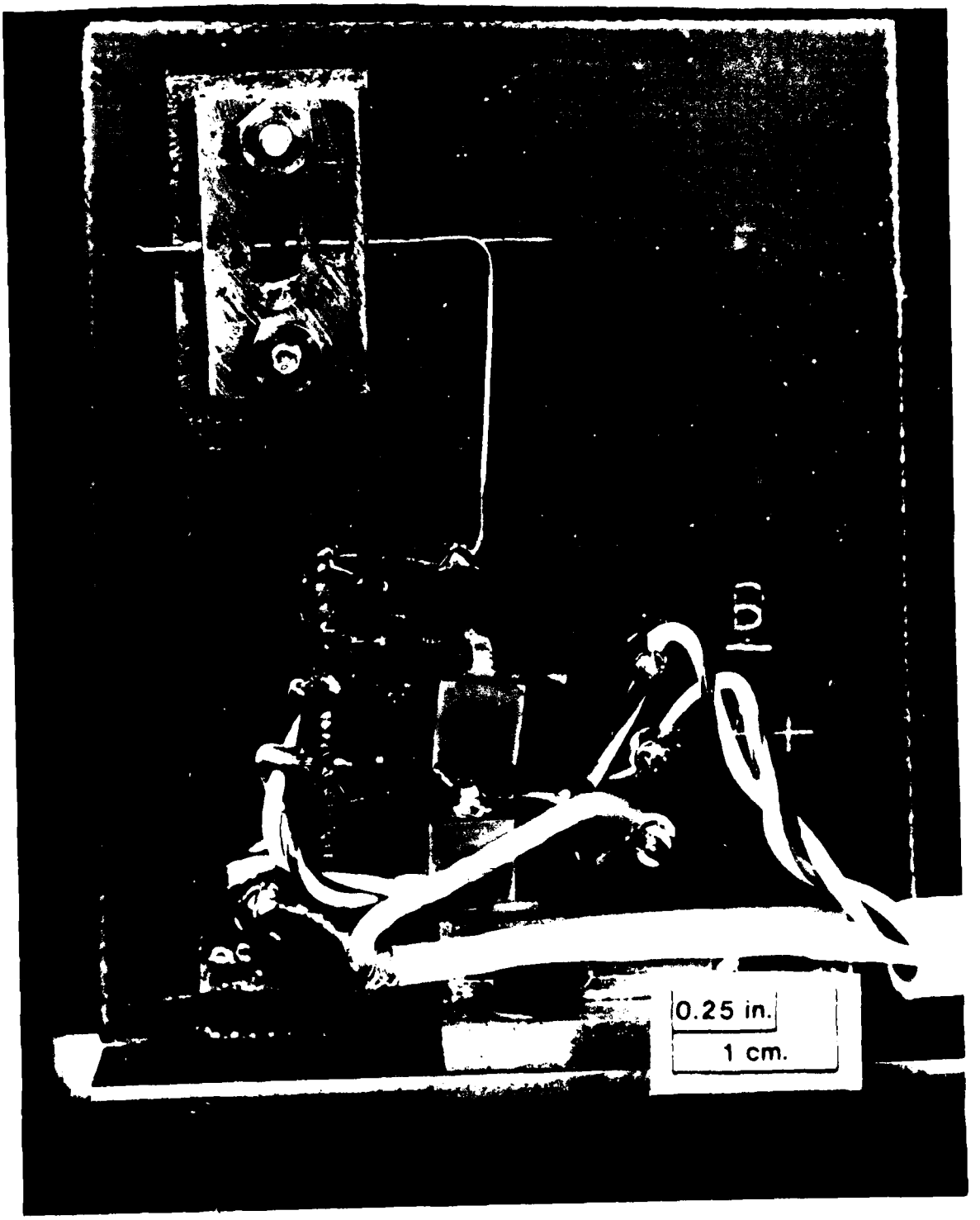

and a separte bttery provides the bias current for the diode. Figure 35 shows the amplifier and bias on-off switches. The detector bias is adjusted by plugging the microampmeter (provided with the detectors) into the jack and adjusting the potentiometer to obtain the desired current level. The bias circuit is current limited to a value well below the damage threshold. The Gates cell is recharged by plugging the charger (one is provided with each module) into the designated jack. Figure 36 is an electrical schematic for the detector module showing the protection diodes, bias circuit and amplifier. Listed below are the parameters of the specific Schottky diodes which were installed in the delivered detector modules.

Diode Voltage Drop

Diode Current	Module #1	Module #2
10μa	.732v	.730v
100μa	.804	.802
1ma	.884	.879
10ma	1.031	1.011
Effective resistance, Rs	8.3Ω	6.7Ω
ΔV (indicates hysteresis in voltage)	.072v	.072v

3.6 Optoacoustic Locking of the CW CO_2 Laser Pump

3.6.1 Introduction - General Theory

To obtain long term stability of an optically pumped FIR laser requires active stabilization of the CO_2 laser pump. Presented is a description of work performed utilizing the optoacoustic effect to lock the CO_2 laser pump at the optimum frequency for conversion of IR (P(20) 9.55 μm) to FIR (466 μm CH_3F) wavelengths.

FIG. 35

TOP VIEW OF SCHOTTKY DETECTOR WITH ACCESS PANEL REMOVED

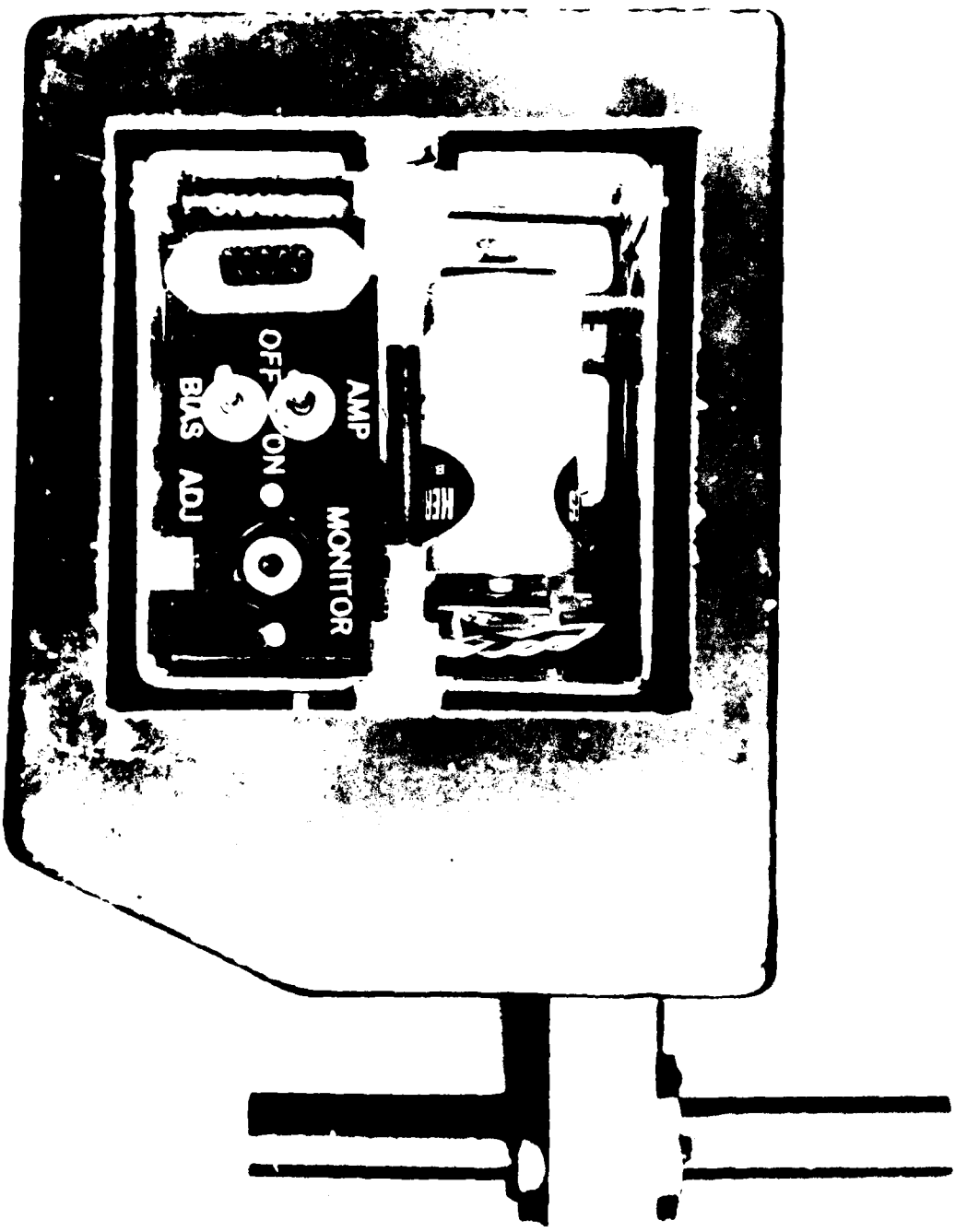

FIG. 36

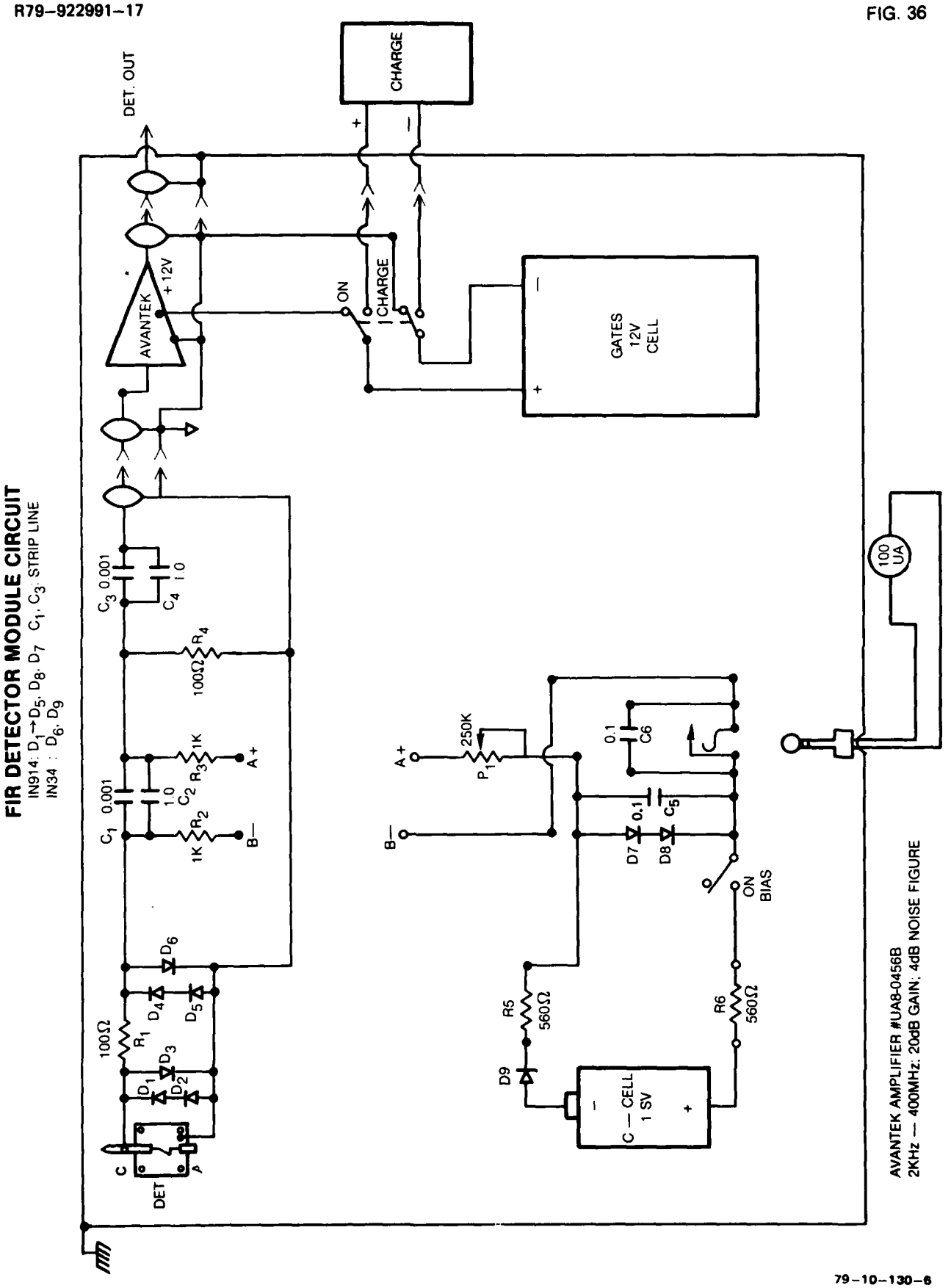
FIR DETECTOR MODULE CIRCUIT
IN914: D1→D5, D8, D7 C1, C3: STRIP LINE
IN34 : D6, D9
DET. OUT
CHARGE
+
—
AVANTEK
+ 12V
ON
CHARGE
GATES
12V
CELL
C3 0.001
C4 1.0
R4
100Ω
1K
R3
A+
C1 0.001
1.0
C2
1K
R2
B—
D6
D4
D5
100Ω
R1
D3
D1
D2
C
A
DET
A+
250K
P1
B—
0.1
C6
D7
0.1
C5
D8
ON
BIAS
R5
560Ω
R6
560Ω
D9
C — CELL
1 SV
100
UA
AVANTEK AMPLIFIER #UA8-0456B
2KHz — 400MHz; 20dB GAIN; 4dB NOISE FIGURE
79-10-130-6

The photoacoustic effect has been known for some 95 years now, and a number of review papers on this subject have been written (Ref. 12-14). The basic concept of the optocacoustic effect is relatively straightforward. When radiation is passed through a closed cell containing an absorbing medium, the pressure of the cell will increase. This pressure change can then be detected with a microphone providing information on the interaction. In the present case, the radiation source is a CO_2 laser and the absorbing medium is approximately 0.5 torr of methyl flouride (CH_3F) located in a 7 cm absorption cell. The signal derived from the interaction occurring in this cell is used in conjunction with phase-sensitive detection techniques to generate an error signal for a feedback control circuit. Prior to this work, this technique has only been used to stabilize the CO_2 pump for the 118 μm transition in methyl alcohol (CH_3OH) (Ref. 15). With the addition of the successful application of this technique to methyl flouride it appears this technique can be generally applied to optimize the pump frequency for many other optically pumped FIR laser transitions.

At this point it is desirable to obtain a more quantitative picture of the optoacoustic effect specifically applied to the interaction of the P (20) line of the 9μm band with CH_3F. In Figure 37 is shown a simplified energy-level diagram of the prolate symmetric top methyl flouride molecule. The laser output at 496μm is due mainly to the pumping provided by the absorption of radiation from the K=2, J=12, V=0 level to the K=2, J=12, V=1 level of the ν_3 vibrational mode. Lasing at 496 μm occurs between the J=12 to J=11 rotational states. The V=1 rotational manifold is depopulated by vibrational to translation energy transfer (V=T), diffusion to and subsequent deactivation at the cell walls, and radiative decay. V=T relaxation is the main process causing the required gas heating for the optoacoustic signal.

A microphone located within the absorption cell will respond to pressure fluctuation within the microphone bandwidth. The rate of pressure change with respect to time can be approximated with the following equation (Ref. 12).

$$\frac{dp}{dt} = 2/3\ \epsilon\ N_1/\tau_c - (P-P_o)/\tau_T \qquad (1)$$

where
- P = time dependent pressure
- P_o = ambient pressure
- ϵ = energy difference between V=0 and V=1
- N_1 = population of the V=1 rotational manifold
- τ_c = V-T relaxation time constant
- τ_T = thermal time constant of absorption cell

SIMPLIFIED ENERGY LEVEL DIAGRAM OF ν_3 MODE OF METHYL ALCOHOL

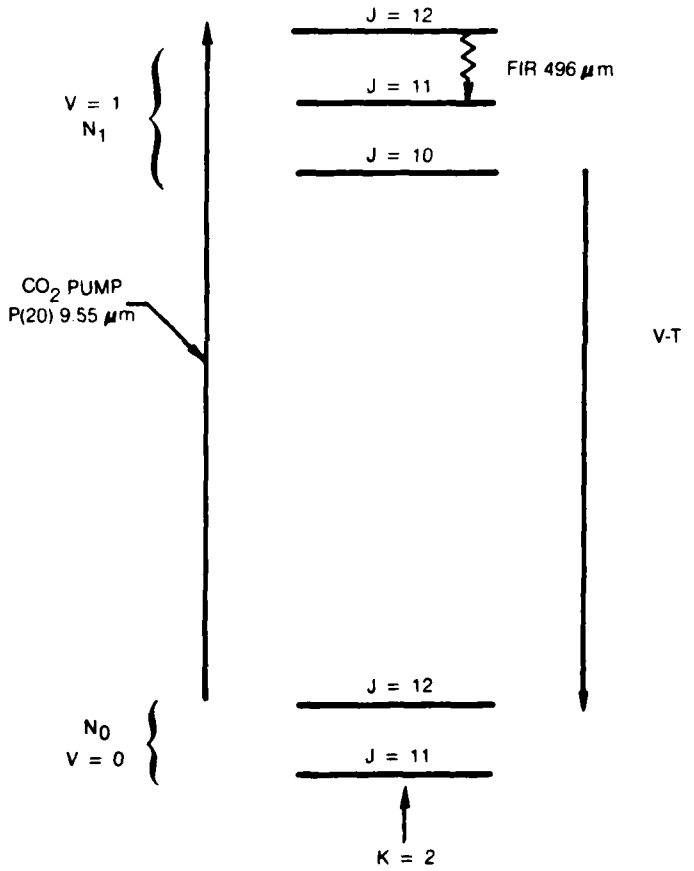

79-08-98-6

An exact solution of this equation does not exist, however, a very simple solution can be obtained if the steady state approximation is invoked. In this case it is assumed that the rate of variation in N_1 is slow compared to τ_c and τ_T, thus

$$\frac{dp}{dt} \approx 0 = 2/3\ \varepsilon\ N_1/\tau_c - (P-P_o)/\tau_T$$

$$P(t) = P_o + \frac{2}{3}\ \varepsilon \frac{\tau_t}{\tau_c} N_1\ (t) \tag{2}$$

From this equation it is seen that the variation in the gas pressure is proportional to the variation in the population N_1.

For the purpose of explaining the g al features of the optoacoustic effect, the following rate equation can b used to determine the N_1 population and is given by

$$\frac{dN_1}{dt} = -N_1\left(\frac{1}{\tau_c} + A\right) + \frac{I\ (N_o\alpha - N_1\beta)A\lambda^2 g(\nu)}{h\nu \qquad 8\pi} \tag{3}$$

where
- N_1 = population of the V=1 rotational manifold
- N_o = population of the V=0 rotation manifold
- α = V=0 rotational partition factor
- β = V=1 rotational partition factor
- ν = pump frequency
- I = pump intensity
- A = A coefficient of N_1
- λ = pump wavelength
- $g(\nu)$ = line shape factor

The solution of this equation can again be easily determined by assuming the steady state approximation. In addition it must be realized that the total number of molecules remains constant, thus

$$N_o + N_1 = N = \text{constant}.$$

Substituting this into equation (2) and applying the steady state approximation yields

$$N_1 = \frac{N\alpha \frac{A\lambda^2}{8\pi h\nu} I(\nu)g(\nu)}{(\alpha+\beta) \frac{A\lambda^2}{8\pi h\nu} I(\nu)g(\nu) + \frac{1}{\tau_c} + A} \quad (4)$$

Making a simple substitution this equation simplifies to

$$N_1 = \frac{N K_1 I(\nu)g(\nu)}{K_2 I(\nu)g(\nu) + \frac{1}{\tau_c} + A} \quad (5)$$

where

$$K_1 = \frac{\alpha A\lambda^2}{8\pi h\nu} \qquad K_2 = \frac{(\alpha+\beta) K_1}{\alpha}$$

It is to be noted in Eq. (5) that the dependence of the N_1 population on the pump laser frequency (ν) comes about through the dependence of the laser intensity and the line shape factor of CH_3F on frequency. A variation in operating frequency ν will provide a variation in the product of $I(\nu)\, g(\nu)$ which causes a variation in N_1 and correspondingly a variation in P (t) given by Eq. (2).

It is the detailed dependence of the $I(\nu)\, g(\nu)$ product on frequency that will determine the optoacoustic signal generated by a small amplitude dither in pump laser frequency. In Fig. 38 is shown the CO_2 laser gain profile, the doppler line shape factor for the methyl flouride absorption band, and a curve proportioned to the product of these two curves (Ref.16). The CO_2 laser gain profile is representative of the actual variation in intensity vs operating frequency obtained with the CO_2 laser used in this study. It is to be noted in this figure that the CO_2 line center is approximately 43 MHz lower in frequency than the absorption line center. This causes the product curve to have a maximum at approximately +18 MHz relative to the CO_2 line center. The present stabilization technique will lock the CO_2 laser at the peak of the product curve. This corresponds to the point of maximum power transfer of CO_2 radiation to the CH_3F molecule and thus optimizes the pump for the production of maximum FIR laser power. This point of lock does not correspond to the line center of either the CO_2 or CH_3F transitions.

Referring to Eq. (5) it can be seen that for very low laser intensities the inequality given by

FIG. 38

CO_2 EMISSION AND CH_3F ABSORPTION LINE SHAPE FUNCTIONS

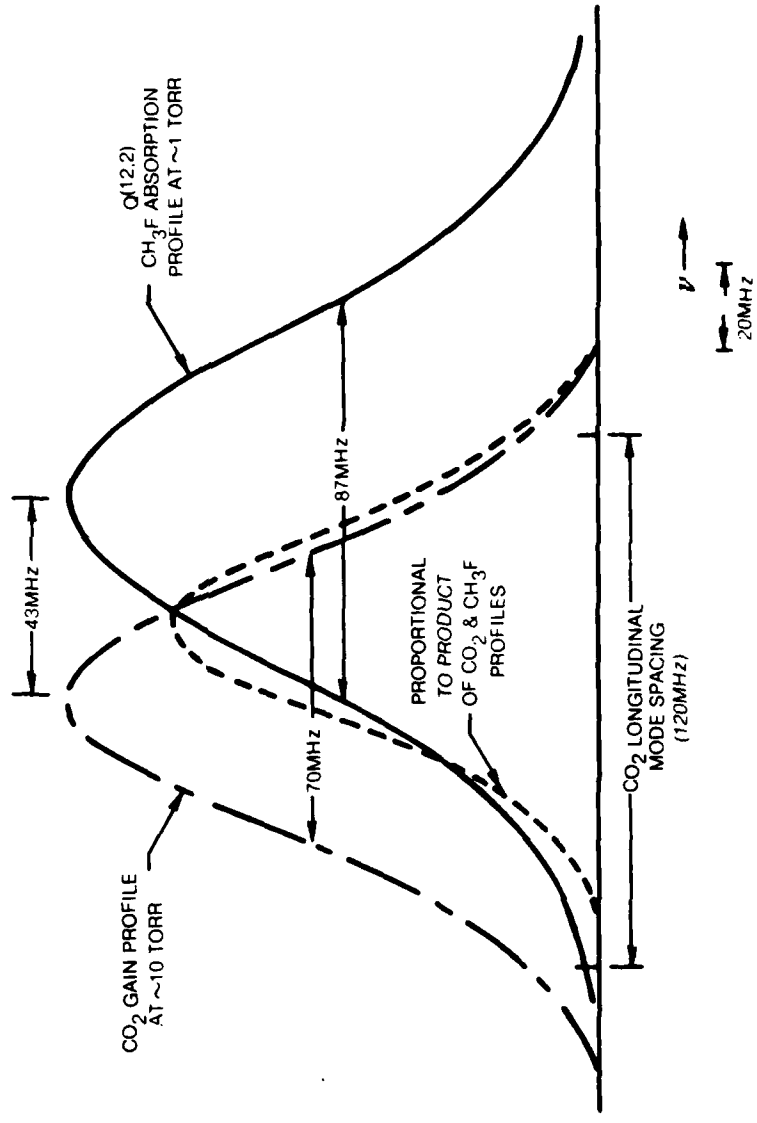

79-08-98-2

$$K_2 I(\nu) g(\nu) \ll \frac{1}{\tau_c} + A \tag{6}$$

will hold. This is the region of linear absorption. Under this condition Eq. (3) simplifies to

$$N_1 = \frac{NK_1 I(\nu) g(\nu)}{1/\tau_c + A} \tag{7}$$

Using this equation in conjunction with the product curve given in Fig. (3) allows one to visualize the optoacoustic signal obtained when the CO_2 laser frequency is dithered. Shown in Fig. 39 is the N_1 population vs. frequency. Under these conditions N_1 is simply proportional to the product of $I(\nu)\, g(\nu)$. Also shown is the N_1 response to an applied dither in laser frequency at three positions of laser oscillation. It is to be noted that the amplitude in the AC component of N_1 is proportional the magnitude of $dn/d\nu$, and the phase of N_1 relative to the applied dither is equal to the sign of $dn/d\nu$.

A microphone located within the absorption cell will respond to the AC component of the N_1 variations which is also shown in Fig. 39. Those familiar with stabilization circuits will recognize this signal as the required error signal for closed loop feedback stabilization. The point of lock is at the null corresponding the maximum N_1 population.

If the laser signal level is not sufficiently small so as to meet the inequality of Eq. (6), then the resulting optoacoustic signal must be interpreted from the more general form of N_1 given in Eq. (5). Taking the opposite case of a very intense field such that

$$K_2 I(\nu) g(\nu) \gg 1/\tau_c + A$$

it found from Eq. (5) that

$$N_1 = \frac{NK_1}{K_2} = N \frac{\alpha}{\alpha+\beta}$$

which is simply a constant. This is the case of a strongly saturated transistion. In this case a dither in CO_2 laser frequency will not yield an optoacoustic signal. Thus under the limits of the present description it is seen that as the intensity of the laser source is increased from very low to very high intensities a maximum in optoacoustic signal will occur. The exception to this is if the CO_2 laser is operating at frequencies corresponding to the peak in the N_1 population shown in Fig. 39 which for any intensity will always yield a null in optoacoustic signal.

FIG. 39

ORIGIN OF OPTOACOUSTIC SIGNAL FOR LOW LASER INTENSITY

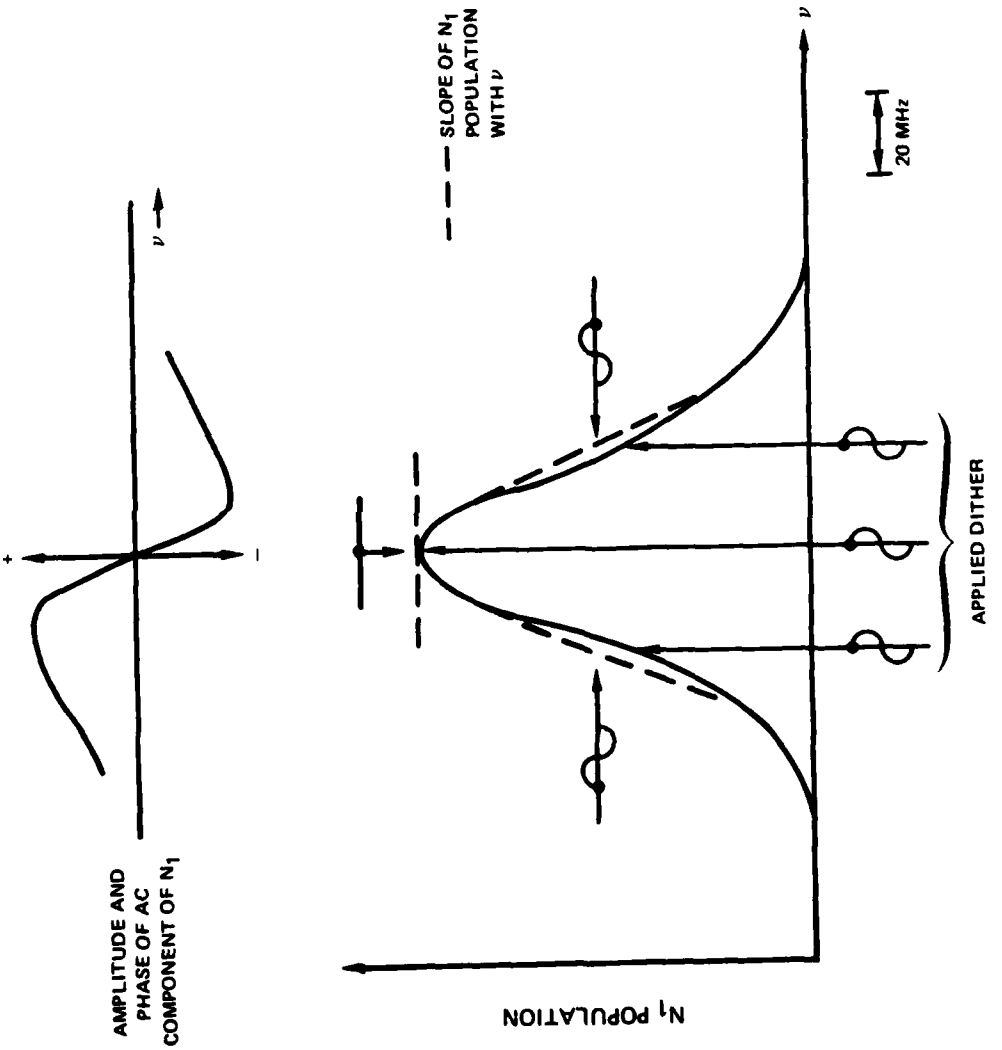

79-08-98-1

From a practical standpoint it is only the general shape of the optoacoustic amplitude and phase curve, as presented in Fig. 39, that is important to realize feedback stabilization of the CO_2 laser pump. As the CO_2 laser is tuned over its gain profile, it is only necessary that optoacoustic signal be of an amplitude well above the noise of the detection system which decreases in value, passes thru a null, and then increases in value but with a reversed phase relative to the applied dither. It has been found experimentally that these conditions can easily be meet for CH_3F even by placing the optoacoustic cell directly at the output of the CO_2 laser where the condition of strong saturation is expected.

3.6.2 Experimental Apparatus and Operation

In Fig. 40 is shown a schematic of the apparatus used for optoacoustic locking experiments. It consists of single mode CO_2 laser operating on P(20) of the 9 μm band whose PZT tuned output is directed through the optoacoustic cell containing .375 torr of CH_3F. The absorption introduced by the cell is less than a percent of the total CO_2 power. After passing through the cell the laser beam enters either a power meter or the FIR laser. If the FIR laser is operative, it is monitored with another power meter.

A block diagram of the electronics used for the locking experiment is shown in Fig. 41. The optoacoustic signal is detected with a Knowles Electronics BT-1759 condenser microphone with an integral FET amplifier. This microphone requires a dc supply voltage of approximately 1.5 volts which is obtained from a flashlight battery. In Fig. 42 are shown details of the optoacoustic cell delivered under this contract and in Fig. 43 is shown the manner in which the supply box (supplied with the cell) is connected to the microphone flange.

Returning to Fig. 41 it is seen that the output of the microphone is connected to the input of an Ithaco lock-in amplifier. The phase sensitive detected signal generated by the lock-in amplifier is sent either to a chart recorder for display or to a Burleigh RC-42 ramp generator - operational amplifier combination for closed loop stabilization of the CO_2 laser. The lock-in amp was typically set at a sensitivity of 3 mv and a time constant of 125 millisec. A reference signal of 100 Hz generated internally by the lock-in was adjusted in amplitude with a potentiometer and then AC couple to the input of the Burleigh RC-42. The 100 Hz reference signal was amplified by 100 resulting in a 34 volt p-p dither signal applied to a Burleigh PZ-80 PZT. This results in a cavity length dither of .27 μm and a CO_2 laser frequency dither of approximately 6 MHz.

If closed loop locking was to be performed, the RC-42 was operated strictly as an operational amplifier. In this case the error signal derived from the lock-in amplifier provided the necessary adjustment in the dc signal applied to the PZT. The phase of the error signal was adjusted with the lock-in to obtain a

FIG. 40

APPARATUS FOR OPTOACOUSTIC LOCKING EXPERIMENT

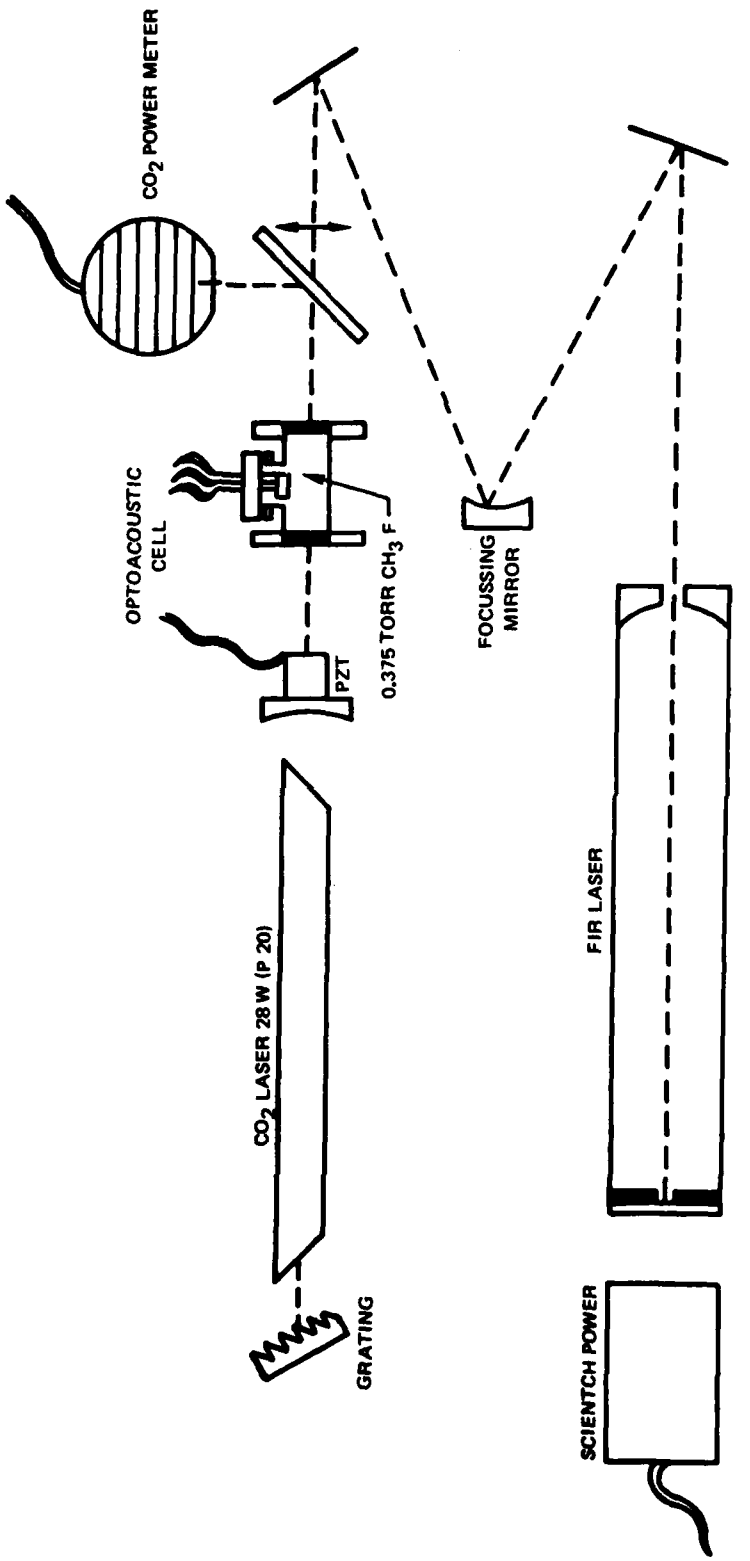

79-08-98-4

FIG. 41

ELECTRONICS FOR OPTO-ACOUSTIC LOCKING EXPERIMENTS

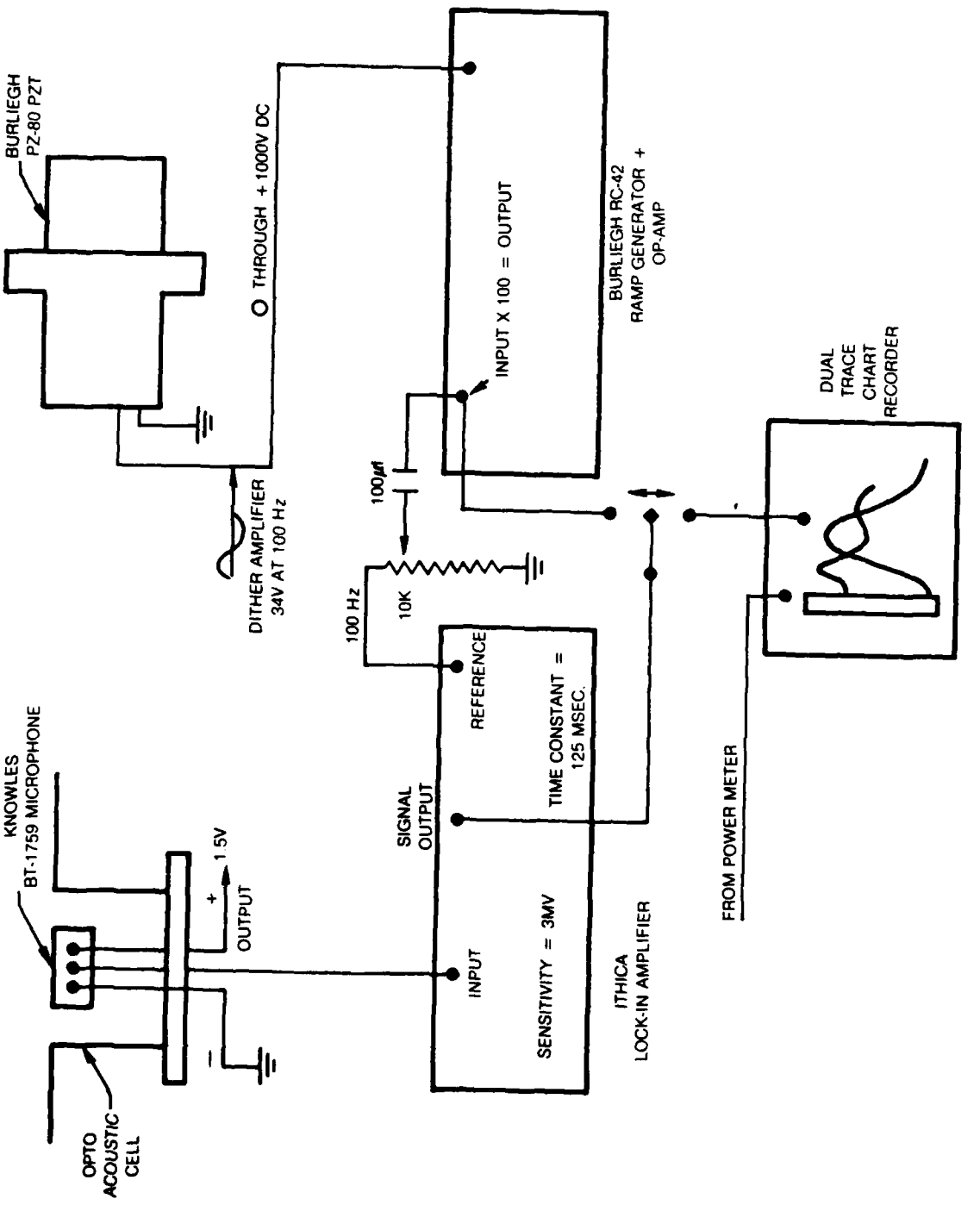

79-08-08-7

FIG. 42

OPTO-ACOUSTIC CELL

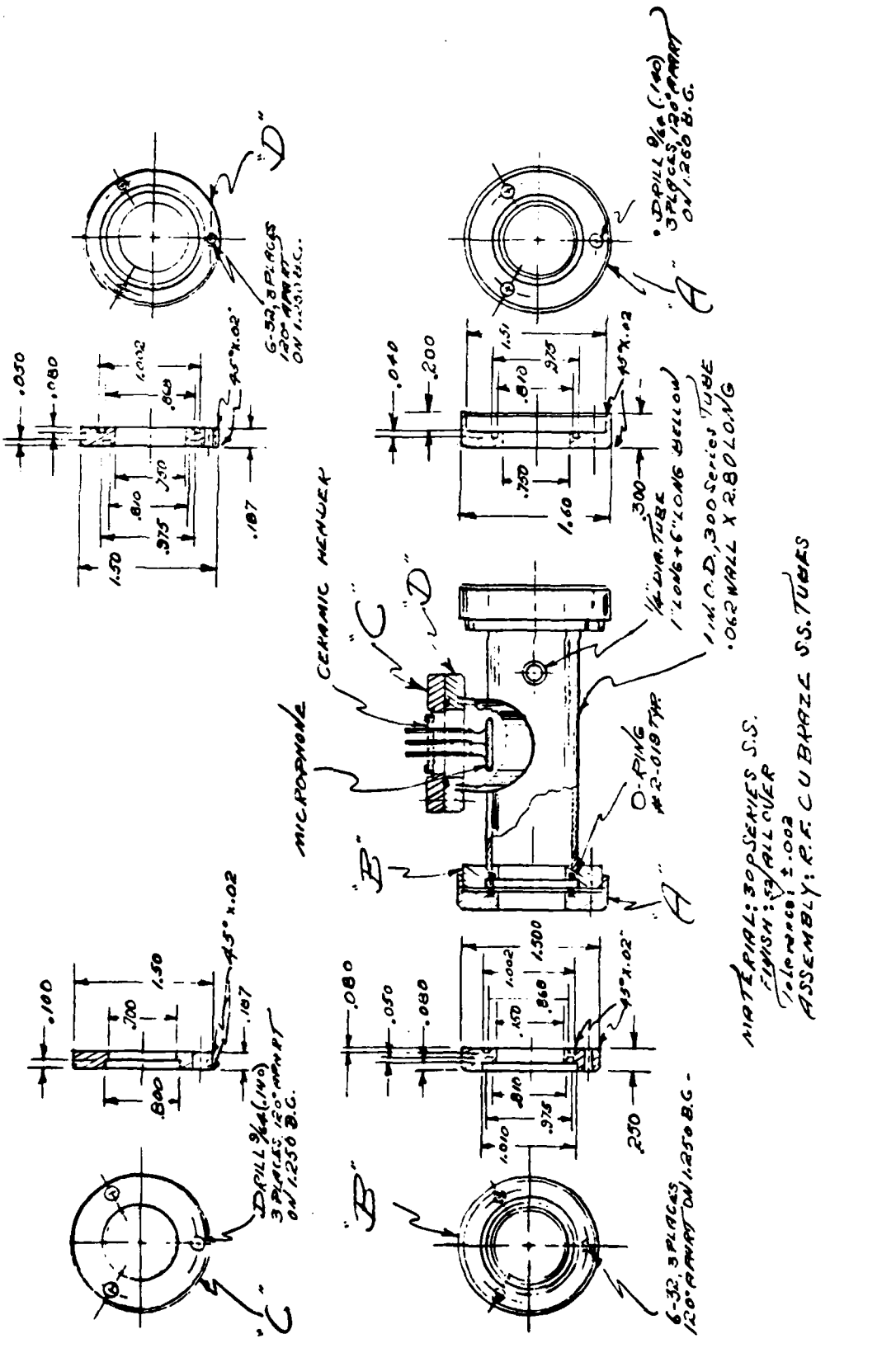

79-08-98-3

FIG. 43

CONNECTION OF SUPPLY BOX TO OPTOACOUSTIC CELL

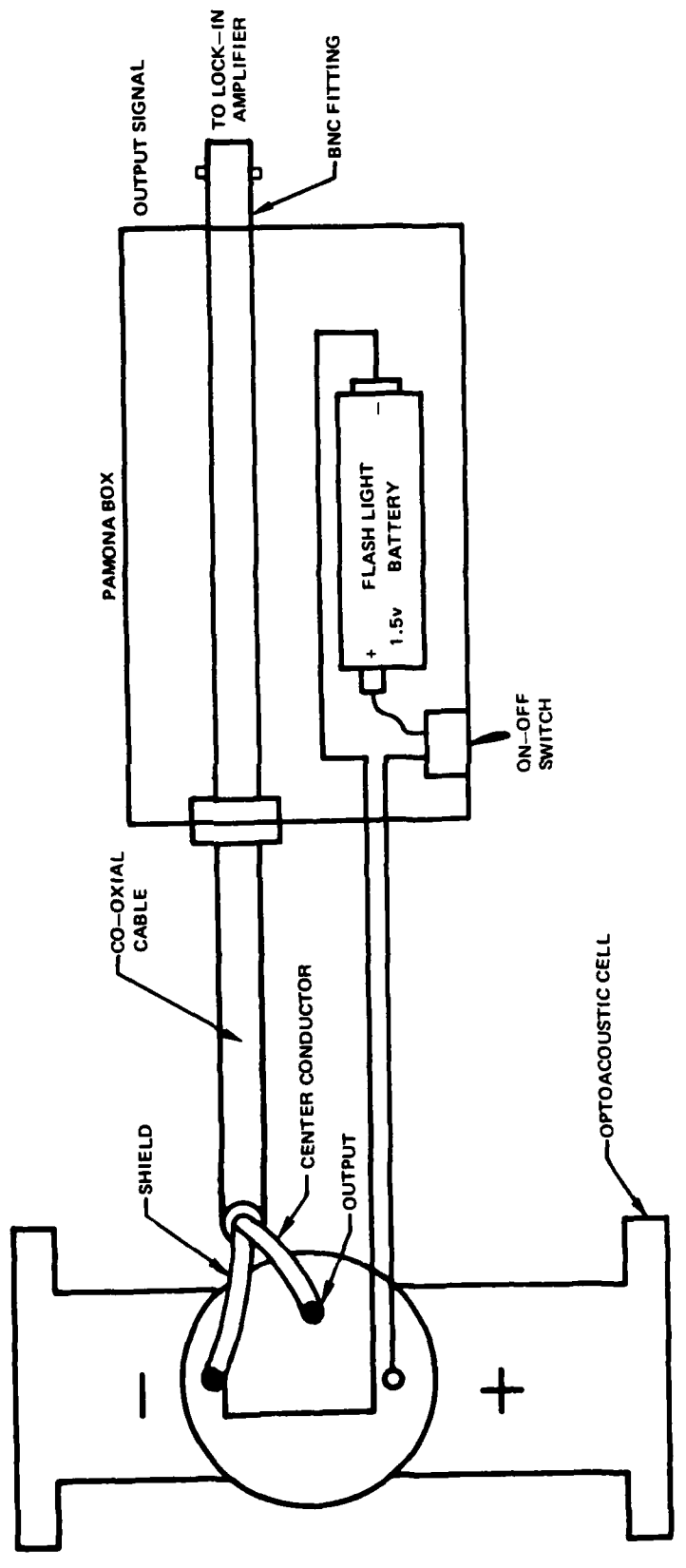

FIG. 42

OPTO-ACOUSTIC CELL

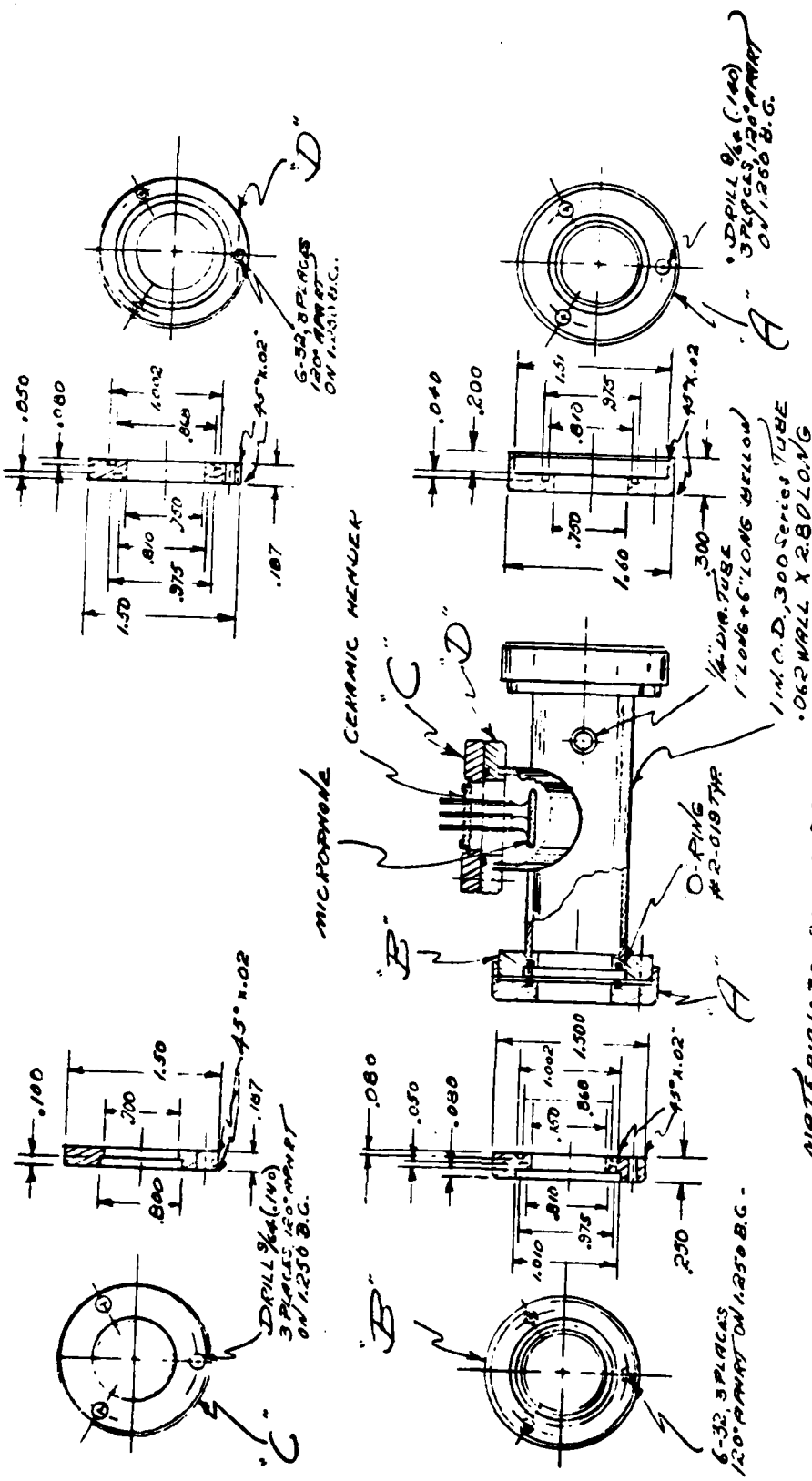

79-08-98-3

stable lock at the null in the optoacoustic signal. If the error signal was to be observed, the lock-in output was displayed on a chart recorder and the RC-42 was used to apply a zero through 1000 volt ramp to the PZT.

It is to be noted that the output of the laser is not the only place the optoacoustic cell could have been positioned. For example the signal coming off of the grating at zero order or the signals derived from the ZnSe Brewster windows could also have been used. In fact these lower level signals should produce a large optoacoustic signal because of the reduction in the effect of saturation mentioned previously.

3.6.3 Experimental Results

The experimental set-up indicated in Figs. 40 and 41 was adjusted to obtain a chart recording of the laser power and the phase-sensitive detected optoacoustic signal as the cavity length was ramped over approximately a 7μm length in a time interval of 50 seconds. The results of this experiment are given in Fig. 44.

A number of points should be noted concerning the CO_2 laser power curve shown in Fig. 44. First note that as the cavity length is increased the laser frequency is decreasing in value. Thus, the left-hand side of the figure is at a higher frequency than the right hand side. Secondly note that the laser power curve is asymmetric relative to line center. It has been determined that this effect is due to thermal adjustments to the effective cavity length due to heating or cooling of intracavity optical components as the laser power is increased or decreased respectively. Finally, the fact that the laser can be turned off by a cavity length adjustment is a good indicator of high mode quality of this laser.

Turning to the optoacoustic curve it is seen that zero signal exists when the laser is turned off thus setting the null level for this curve. As the laser starts to oscillate, the intensity is very low, however, a very sizeable optoacoustic signal exists. As the laser intensity increases the optoacoustic signal increases until the laser reaches a power of about 3 watts. At this point the laser is approximately +40 MHz off of line center. The decrease in signal after this point for at least the next ten MHz is attributable to the effects of saturation rather than a decrease in the slope of the $I(\nu)\ g(\nu)$ curve. As the laser frequency is decreased further the optoacoustic signal decreases, passes through a null, then reverses sign and increases in value. The point of lock will occur at the null in optoacoustic signal when the stabilization loop is closed. Note that the null occurs at the +20 MHz relative to the CO_2 line center. This value is in good agreement with the predicted value of +18 MHz indicated previously.

FIG. 44

OPTO-ACOUSTIC SIGNAL VS. CAVITY LENGTH

(a) PHASE-SENSITIVE DETECTED OPTO-ACOUSTIC SIGNAL FROM THE ABSORPTION CELL VS. CO_2 LASER FREQUENCY

(b) CO_2 LASER OUTPUT VS. CAVITY

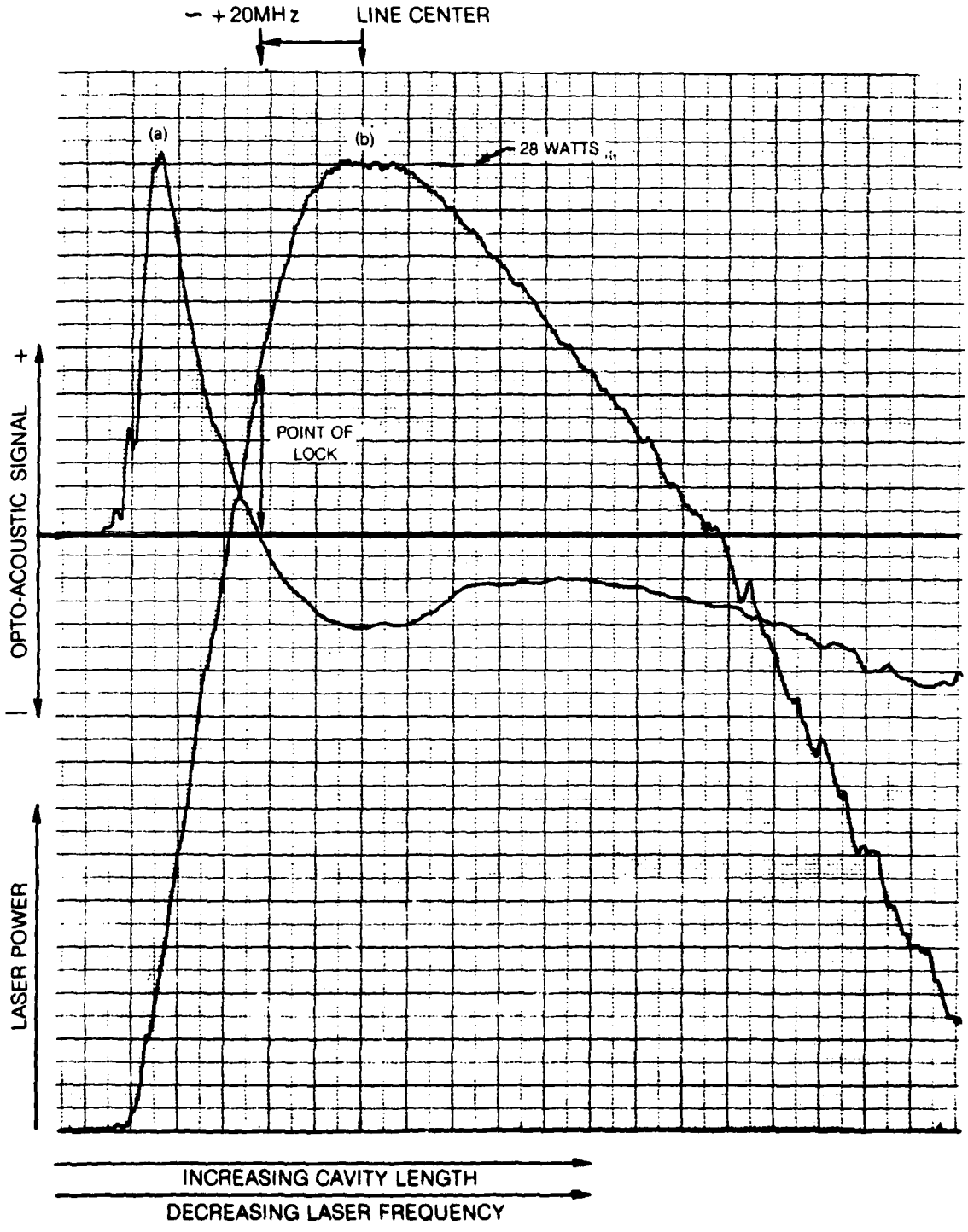

79-08-98-9

In another experiment the CO_2 laser pump was allowed to excite the FIR waveguide laser operating at 496 μm. The output of the FIR laser was monitored as the CO_2 cavity length was adjusted. As expected the maximum FIR output occurs when the optoacoustic signal was nulled or when the stabilization loop was closed.

Finally the long term stability of the output power of a Methyl Alcohol FIR laser operating at 118 μm was monitored under the conditions of an optoacoustic locked or unlocked pump laser. The results of this 48 min duration experiment are presented in Fig. 45. As is obvious from this curve the locked pump laser produces a much more stable FIR output than does the unlocked case. This experiment was not be repeated for CH_3F, but similar results are expected.

It can be concluded from these results that the optoacoustic effect represents a very simple but effective means of stabilizing CO_2 pump lasers at the optimum frequency for IR to FIR conversion in optically pumped FIR laser systems.

FIG. 45

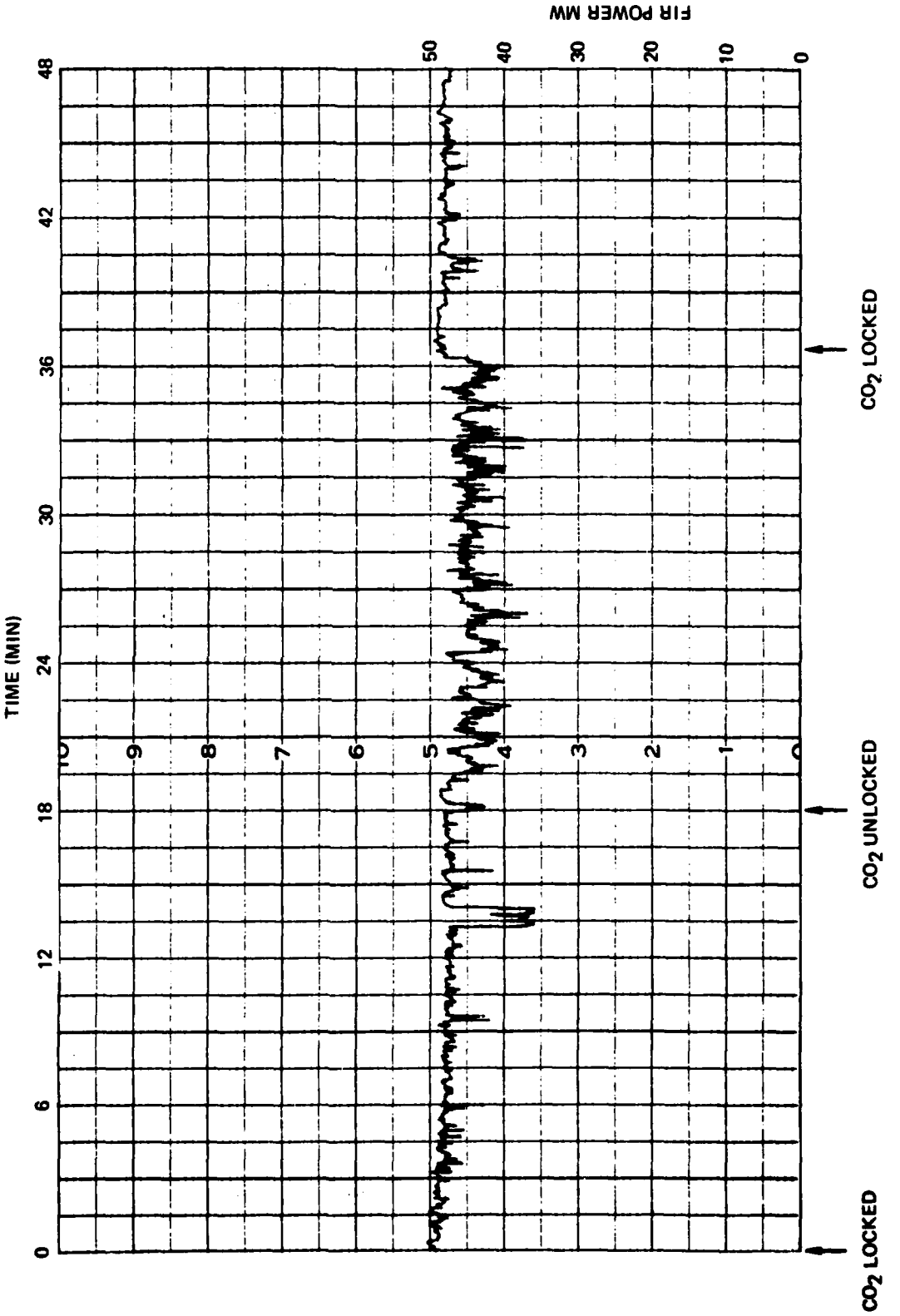
118μ FIR OUTPUT POWER VS LOCKED AND UNLOCKED CO_2 LASER
FIR POWER MW
50
40
30
20
10
0
TIME (MIN)
48
42
36
30
24
18
12
6
0
10
9
8
7
6
5
4
3
2
1
0
CO_2 LOCKED
CO_2 UNLOCKED
CO_2 LOCKED
79-09-96-8

4.0 REFERENCES

1. Wayne, R. J, L. M. Laughman, P. P. Chenausky and C. J. Buczek: Pulsed Laser Transmitter, Final Technical Report, No. R77-922618-9 under Contract N60921-76-C-0200 with Naval Surface Weapons Center, October 1977.

2. Stark, D. S., P. H. Cross and M. R. Harris: A Sealed UV-pre-ionisation CO_2 TEA Laser with High Peak Power Output. J. Physics E: Sci. Instru., Vol. 11 (1978).

   Stark, D. S. and M. R. Harris: Platinum-Catalyzed Recombination of CO and O_2 in Sealed CO_2 TEA Laser Gaser. J. Physics E: Sci. Instrum. Vol. 11 (1978).

3. Clobes, A. R.: Pulsed Laser Transmitter System. United Technologies Research Center, Final Technical Report, No. R75-921840-12, under Contract N60921-74-C-0174 with Naval Surface Weapons Center. November 1974.

4. Rosenbluh, M., R. J. Temkin and K. J. Button: Submillimeter Laser Wavelength Tables. Applied Optics, Vol. 15, p. 2635 (1976).

5. Yamanaka, M.: Optically Pumped Waveguide Lasers. J. Opt. Soc. Am., Vol. 67, p. 952 (1977).

   Koepf, G. A. and N. McAvoy: Design Criteria for FIR Waveguide Laser Cavities. IEEE J. Quantum Electron, Vol. 2E-13, p. 418 (1977).

6. Mirrors were fabricated and coated by Laser Optics, Inc., P.O. Box 127, Danbury, Connecticut 06810.

7. Replica grating on metal substrate was purchased from Bausch and Lomb, Inc. Rochester, New York. Grating catalog number 35-53-06-890.

8. Fahlen, T. S.: CO_2 Laser Design Procedure. Applied Optics, Vol. 12, p.2381 (1973).

9. Pyroelectric Detectors Used Were: (1) Laser Precision, Inc. model KT-1510; (2) Molectron, Inc. Model P1-61.

10. Dr. Robert Mattauch, Department of Electrical Engineering, School of Engineering and Applied Science, Thornton Hall, University of Virginia, Charlottesville, Virginia 22901.

11. Twu, B. and S. E. Schwarz, Properties of Infrared Cat-Whisker Antennas Near 10.6μ Applied Physics Letters, Vol. 26, p. 672 (1975).

REFERENCES (Cont'd)

12. Kreuzer, L. B.: Ultralow Gas Concentration Infrared Absorption Spectroscopy JAP Vol. 42, #7, p. 2934 (1971).

13. Rosengren, L. G.: A New Theoretical Model of the Optoacoustic Gas Concentration Detector. Infrared Physics, Vol. 13, p. 109 (1973).

14. Rosengren, L. G.: Optimal Optoacoustic Detector Design. Applied Optics, Vol. 14, #8.

15. Busse, G., E. Basel, and A. P. Faller, Appl. Phys., Vol. 12, p. 387 (1977).

16. Plant, T. K.: High Power Optically Pumped for Infrared Laser Sources. Ph.D. Thesis, University of Illinois at Urbona-Champaign (1975).